ISTANBUL TECHNICAL UNIVERSITY ★ ENERGY INSTITUTE

DEVELOPMENT OF A NODAL METHOD FOR THE SOLUTION OF THE NEUTRON DIFFUSION EQUATION IN CYLINDRICAL GEOMETRY

M. Sc. Thesis by

Mehmet MERCİMEK, Nuclear E. Eng.

Department: **Energy Science and Technology**

Programme: **Energy Science and Technology**

JUNE 2008

ISTANBUL TECHNICAL UNIVERSITY ★ ENERGY INSTITUTE

DEVELOPMENT OF A NODAL METHOD FOR THE SOLUTION OF THE NEUTRON DIFFUSION EQUATION IN CYLINDRICAL GEOMETRY

M. Sc. Thesis by
Mehmet MERCİMEK, Nuclear E. Eng.
(301061015)

Date of submission: 5 May 2008

Date of defence examination: 10 June 2008

Supervisor (Chairman): Prof. Dr. Atilla ÖZGENER

Members of the Examining Committee: Prof. Dr. Melih GEÇKİNLİ (I.T.U.)

Prof. Dr. Cemal YILDIZ (I.T.U.)

JUNE 2008

İSTANBUL TEKNİK ÜNİVERSİTESİ ★ ENERJİ ENSTİTÜSÜ

SİLİNDİRİK GEOMETRİDE NÖTRON DİFÜZYON DENKLEMİNİN ÇÖZÜMÜ İÇİN NODAL BİR YÖNTEM GELİŞTİRME

YÜKSEK LİSANS TEZİ
Nükleer E. Müh. Mehmet MERCİMEK
(301061015)

Tezin Enstitüye Verildiği Tarih: 5 Mayıs 2008
Tezin Savunulduğu Tarih: 10 Haziran 2008

Tez Danışmanı: **Prof. Dr. Atilla ÖZGENER**

Diğer Jüri Üyeleri: **Prof. Dr. Melih GEÇKİNLİ (İ.T.Ü.)**

Prof. Dr. Cemal YILDIZ (İ.T.Ü.)

HAZİRAN 2008

FOREWORD

Nodal methods are fast and accurate methods which combine attractive features of the finite element method as well as of the finite difference method. In this work, a nodal method has been developed in cylindrical geometry which gives acceptably accurate results for realistic problems.

I would like to express my sincere gratitude to my supervisor Prof. Dr. Atilla ÖZGENER. His invaluable knowledge, expert guidance and care allowed this work to be completed.

Special thanks and appreciation go to Prof. Dr. Bilge ÖZGENER and Prof. Dr. Akif ATALAY for their great support, advice and time.

I also wish to thank my colleagues from Istanbul Technical University Institute of Energy; especially physics engineer and ITU TRIGA MARK II reactor operator Mehmet GENCELİ for his guidance, support and encouragement.

I would also like to recognize my dear friends Abdülhamit ERTUNGA, Erdal KEKLİK, Ramazan AKYÜZ for helping me in their own unique ways.

Finally I would like to thank my parents, Mehmet and Yüksel MERCİMEK, my dear brother Mustafa MERCİMEK and my sister Serpil MERCİMEK for encouraging me throughout my life.

June 2008 **Mehmet MERCİMEK**

TABLE OF CONTENTS

LIST OF ABBREVIATIONS

FEM	: Finite Element Method
NEM	: Nodal Expansion Method
ODE	: Ordinary Differential Equation
RHS	: Right Hand Side
1-d, 2-d	: One-Dimensional, Two-Dimensional

LIST OF TABLES

Page Number

LIST OF FIGURES

Page Number

LIST OF SYMBOLS

$\vec{J}_g(\vec{r})$	: Neutron current density vector for group g
$\mathbf{D^g}$	: Diffusion coefficient for group g
ϕ_g	: Neutron flux for group g
$\mathbf{\Sigma_r}$	: Macroscopic removal cross-section
$\mathbf{\Sigma_a}$	: Macroscopic absorption cross-section
$\mathbf{\Sigma_{s,g\rightarrow g'}}$	: Macroscopic scattering cross-section from group g to group g'
$\mathbf{\Sigma_f}$	: Macroscopic fission cross-section
$\mathbf{k_{eff}}$	: Effective multiplication factor
$\boldsymbol{\chi}$	: Fission spectrum
$\boldsymbol{\nu}$	: Average number of neutrons released per fission
$\mathbf{Q}$	: Neutron source
$\mathbf{r_{i-1/2}, r_{i+1/2}, r_i}$	: Radii at node edges and center respectively
$\mathbf{\Delta_i}$	: i^{th} node width
$\mathbf{j^+}$	: Right-going partial current
$\mathbf{j^-}$	: Left-going partial current
$\mathbf{S_{i+1/2}, S_{i-1/2}, S_i}$	: Surface areas at node edges and center respectively
$\mathbf{P_l}$	: l^{th} order polynomial
ξ	: Local variable
$\mathbf{a_l}$	: Expansion coefficients for polynomial of l^{th} order
$\underline{\underline{A}}_1^{(3x3)}$	: 3 by 3 matrix constituted from one node formulation
$\underline{\underline{0}}^{(3x3)}$	: 3 by 3 matrix with all elements are zero
$\boldsymbol{\varepsilon}$	: Convergence parameter
$\mathbf{B}$	: Buckling term
$\mathbf{J_0, J_1}$	: Bessel functions of first kind, zeroth and first order respectively
$\mathbf{w_f}$	: Recoverable energy per fission
$\bar{\phi}$	: Average flux
$\boldsymbol{\lambda}$	: Maximum eigenvalue, k_{eff}
$\mathbf{I_0, K_0, I_1, K_1,}$	: Zeroth and first order modified Bessel functions of first and second kind respectively

SİLİNDİRİK GEOMETRİDE NÖTRON DİFÜZYON DENKLEMİNİN ÇÖZÜMÜ İÇİN NODAL BİR YÖNTEM GELİŞTİRME

ÖZET

Nükleer reaktörlerin birçok fiziksel özelliği nötron difüzyon teorisi ile anlaşılmaktadır. Difüzyon teorisinin geçerli olabilmesi için reaktör ortamını oluşturan binlerce küçük malzeme, ortalama tesir kesitleri ve difüzyon katsayıları kullanılarak homojenleştirilir.

Bu homojenleştirme işlemine rağmen reaktör kalbi yine de oldukça heterojen bir ortam oluşturur. Bu heterojenlik yakıt demetleri arasındaki yakıt miktarları farkından, yanıcı zehirlerden, kontrol çubuklarından, su kanallarından, yapısal malzemelerden vs. kaynaklanır.

Geleneksel sonlu farklar yönteminde ağ aralığı iki gereksinimi karşılayacak şekilde seçilmelidir: (a) kalan heterojenliği gösterebilmeli (b) termal difüzyon uzunluğundan daha kısa olmalı.

Böyle bir sonlu farklar modeli 100.000 - 1.000.000 kadar bilinmeyen içerir. Bu ise bilgisayar donanımında ki gelişmeye rağmen ürkütücü bir problemdir.

Bunun yerine reaktör kalplerinde nötron akı dağılımını ve etkin çoğaltma katsayısını bulmak için çok sayıda yaklaşım yöntemi geliştirilmiştir. Bunlar nodal, kaba ağ ve sentez yöntemleri olarak sınıflandırılır.

Nodal yöntemlerde, reaktör kalbi nod denilen büyük homojenleştirilmiş alanlara bölünür. Genellikle bir yakıt topluluğu (asemble) ya da toplulukları bir nod olarak tanımlanır. Böylece bilgisayar zamanından ve depolama alanından kazanılır. Nodal hesaplamalar sonucu bir yakıt topluluğu için güç ya da ortalama akı ve reaktör için etkin çoğaltma katsayısı bulunur.

Nodal yöntemlerin temel fikri iki nod arasındaki yüzeyde nötron akımları ve bu nodlarda ortalama nötron akıları arasında ilişki kurmaktır. Bu ilişkiyi sağlayan bir katsayı matrisi oluşturulur.

Geleneksel ve dik yönde integre edilmiş nodal yöntemler olmak üzere birbirinden oldukça farklı iki sınıf nodal yöntem geliştirilmiştir. Her ikisi de aynı nodal denge denklemini kullanmalarına rağmen ayrık sistemi çözecek ek denklemleri farklı şekilde türetirler. Bu tezin teorik temelini dik yönde integrasyon yaparak elde edilen nodal açılım yöntemi oluşturur.

Bu çalışmada polinom açılım yöntemlerinden biri olan nodal açılım yöntemlerinden en düşük dereceden olanı kullanılmıştır. Sistem geometrisi olarak bir boyutlu silindir alınmıştır. Açılım katsayılarının bulunmasında Fick Yasasından, ayrık nodal denge denkleminden ve normal akımın sürekliliğinden yararlanılmıştır. Her bir nod için ikisi Fick Yasasından biri ayrık nodal denge denkleminden olmak üzere üç denklem ya da bir başka ifadeyle üç vektör elde edilmiştir. Bu denklemler bir katsayı matrisini oluştururlar.

Çok gruplu difüzyon teorisi için yetkinlik-özdeğer hesaplamaları yapabilen bir bilgisayar programı bu matris formundan yararlanılarak geliştirilmiştir. Bu program FORTRAN 90 dilinde yazılmış ve WINDOWS işletim sisteminde koşulmuştur. Derleyici olarak FORTRAN Power Station 4.0 kullanılmıştır. Bu program çok gruplu nötron difüzyon denklemini çok bölgeli bir sistem için çözerek etkin çoğaltma katsayısını, akı ve akım dağılımını ve ortalama akımları bulma yeteneğine sahiptir. Bu FORTRAN programının ismi olarak, R yönünde nodal açılım yöntemi kelimelerinin İngilizce baş harflerinden oluşan NEMR seçilmiştir.

NEMR programını doğrulamak için bir gruplu, bir grup iki bölgeli, iki gruplu problemlerin analitik çözümleri bulunmuş, bu sonuçlar hem NEMR programının sonuçları ile hem de lineer ve kuadratik sonlu elemanlar yöntemi ile karşılaştırılmıştır. Sonlu elemanlar yöntemi için QFEMR programı kullanılmıştır. Son olarak iki grup çok bölgeli bir reaktör olan TRIGA reaktörü için program koşulmuş ve bütün bu problemlerde NEMR programının tutarlı ve doğru sonuçlar verdiği gözlenmiştir.

Bu tezin amacı sonsuz silindirik bir ortam için nodal yöntem programı geliştirmek ve nodal yöntemler ile sonlu elemanlar yöntemini karşılaştırmak, hangi yöntemin hangi durumlarda daha iyi sonuç verdiğini gözlemlemek olmuştur. Test problemlerinden görüleceği gibi bilgisayar programı doğrulanmış ve geliştirilen nodal yöntemin sonlu elemanlar yöntemlerine göre nod sayısının oldukça az olduğu kaba ağlarda daha iyi sonuçlar verdiği görülmüştür.

DEVELOPMENT OF A NODAL METHOD FOR THE SOLUTION OF THE NEUTRON DIFFUSION EQUATION IN CYLINDRICAL GEOMETRY

SUMMARY

Diffusion theory is sufficiently accurate to provide a quantitative understanding of many physics features of nuclear reactors. A homogenized mixture with average cross-sections and diffusion coefficients are used to create a computational model for which diffusion theory is valid.

Even after assembly homogenization, the reactor core remains a highly heterogeneous medium because of assembly-to assembly variation in fuel composition, burnable poisons, control rods, water channels, and structure and so on.

The mesh spacing in a conventional few-group finite difference model of the core is constrained by two requirements: (a) Representation of the remaining heterogeneity (b) it must be shorter than thermal diffusion length.

Such finite difference model requires 100,000 to 1,000,000 unknowns. This is a formidable problem even today despite tremendous advances in computer hardware.

A large number of approximation methods has been developed to enable a more computationally tractable solution for the effective multiplication constant and neutron flux distribution in reactor cores. These methods can be classified as nodal, coarse-mesh and synthesis methods.

In nodal methods, the reactor core is subdivided into large homogenized regions and each such region constitutes a node. Usually a subassembly (or sometimes a group of assemblies) is defined as a node. Nodal calculations are carried out to determine the effective multiplication factor and assembly powers (or assembly average fluxes).

The essential idea of nodal methods is to relate neutron currents across an interface between two nodes to the average flux levels in those two nodes; that of the coefficient matrix is to relate the fluxes and currents on the nodal surfaces directly to each other.

Two rather distinct classes of nodal methods have evolved; conventional and transverse integrated. They have a common foundation in the discrete nodal balance equation and are characterized by the techniques they employ to derive the additional equations necessary to solve the discrete system. Transverse integrated nodal expansion method constitutes the theoretical basis of this thesis.

In this work, a lowest order nodal expansion method has been developed in one dimensional cylindrical geometry. The expansion coefficients are determined by applying Fick's law in combination with discrete nodal balance equation and continuity of normal current. Three equations for each node are obtained. Nodal balance equation constitutes one equation and other two equations are derived from Fick's law. These equations are used to form a coefficient matrix.

A computer program which can carry out criticality-eigenvalue calculations in multi-group diffusion theory is developed using this matrix form. The program has been

written in FORTRAN 90 and run in WINDOWS operating system. It is compiled in FORTRAN Power Station Version 4.0. It is capable of calculating effective multiplication factor, flux and current distribution, average fluxes for multi-group and multi-region problems. It has been named NEMR (Nodal Expansion Method in R direction)

In order to validate this program, it was run for the problems with known analytical solutions. Results were compared with calculated values and finite element method solutions which were obtained using a FORTRAN program called QFEMR. (Quadratic Finite Element Method in R direction)

Four problems extend from a simple bare, one group reactor to two-group, seven-region TRIGA reactor were cosidered. Effective multiplication factors, flux distributions and average fluxes were compared with analytical solutions.

The objective of this thesis has been to develop a nodal method program for infinite cylinder and compare nodal and finite elements methods. It has been seen from the benchmarking problems that this aim has been accomplished. Nodal expansion method and quadratic finite element method were shown to be of better accuracy with respect to linear finite element method. It also appears that nodal expansion method is a practical method for the problems in which the mesh is very coarse.

1 INTRODUCTION

1.1 Diffusion Theory

In order to design a nuclear reactor properly, it is necessary to be able to predict how the neutrons will be distributed throughout the system. The approximate value of the neutron distribution can be found by solving the diffusion equation, essentially the same equation as is used to describe diffusion phenomena in other branches of engineering. This procedure was used for the design of most early reactors and it is still widely used to provide first estimates of reactor properties [1].

Diffusion theory provides a strictly valid mathematical description of the neutron flux when the assumptions made in its derivation - absorption much less likely than scattering, smooth spatial variation of the neutron distribution, isotropic or linearly anisotropic scattering - are satisfied. The first condition is satisfied for most of the moderating and structural materials found in a nuclear reactor, but not for the fuel and control elements. The second condition is satisfied a few mean free paths away from the boundary of large (relative to the mean free path) homogeneous media with relatively uniform source distributions. The third condition is satisfied for scattering from most nuclei.

A modern nuclear reactor consists of thousands of small elements, many of them highly absorbing with dimensions on the order of a few mean free paths or less. Yet diffusion theory is widely used in nuclear reactor analysis and makes accurate predictions. The many small elements in a large region are replaced by a homogenized mixture with effective averaged cross sections and diffusion coefficients, thus creating a computational model for which diffusion theory is valid.

Even after the local fuel pin, clad, coolant, and so on, heterogeneity is replaced by a homogenized representation; a reactor core remains a highly heterogeneous medium because of the intra-assembly and assembly-to-assembly variation in fuel composition, burnable poisons, control rods, water channels, structure and so on [2].

One not only must consider nonuniformities corresponding to fuel pellets, cladding material, moderator, coolant, control elements, but spatial variations in fuel and

coolant densities due to nonuniform core power densities and temperature distributions as well. Such complexities immediately force one to discard analytical methods in favor of a direct numerical solution of the diffusion equation. In fact even when an analytical solution of the diffusion equation is possible, it is frequently more convenient to bypass this in favor of a numerical solution, particularly when the analytical solution may involve numerous functions that have to be evaluated numerically in any event, or when parameter studies are required that may involve a great many such solutions [3].

1.2 Numerical Methods for Solving the Neutron Diffusion Equation

The general procedure is to rewrite the differential diffusion equation in finite difference form and then solve the resulting system of difference equations on a digital computer. The mesh spacing in a conventional few group finite-difference model of a reactor core is constrained by two requirements:

- It must be sufficiently fine to represent the remaining spatial heterogeneity
- It must be no larger than the shortest (thermal) group diffusion length in order to avoid numerical inaccuracy

A few group finite difference model that could adequately describe such a core might well have 100,000-1,000,000 unknowns (the fluxes in each group at each mesh point). The direct solution of such a problem, even in diffusion theory, remains a formidable computation. For calculations such as fuel burnup or transient analysis, in which many full-core spatial solutions are needed, direct few group finite-difference solutions remain impractical.

A large number of approximation methods have been developed to enable a more computationally tractable solution for the effective multiplication constant and neutron flux distribution in nuclear reactor cores. Following historical precedent, these methods can generally be classified as nodal, coarse-mesh and synthesis methods, although distinction among categories may be largely a matter of perspective and sequencing of calculational steps [2].

1.3 Nodal Methods

In order to avoid the large storage and execution time requirements of a direct finite difference treatment of the diffusion equation a scheme is provided by so called nodal methods. The general idea is to decompose the reactor core into relatively large subregions or node cells in which the material composition and flux are assumed uniform. One then attempts to determine the coupling coefficients characterizing node cell leakage and then to determine the node cell fluxes themselves [3].

If the number of nodal cells N is large, the nodal method becomes equivalent to the finite difference scheme and hence loses any calculational advantages. The real power of the nodal approach is realized only when the number of node cells N is small, since then the cells are large enough that they become coupled via neutron diffusion only to nearby cells, that is the transfer matrix is sparse [3].

Usually a subassembly (or sometimes a group of assemblies) is defined as a node so typical dimension of a node cell is in the order of ~20 cm in a nuclear reactor. Nodal calculations are carried out to determine the effective multiplication factor and assembly powers (or assembly average fluxes). Nodal methods are classified further into two distinct categories: conventional nodal methods and transverse integrated nodal methods.

Conventional nodal methods are based on the calculation of a nodal average flux or fission rate for each homogenized subassembly. Neutron diffusion between adjacent nodes is represented by coupling coefficients which are usually determined by empirical means. Conventional nodal methods are also called simulators and can achieve impressive accuracy for the particular reactor type they were intended. Due to the lack of theoretical foundation in conventional nodal methods, researchers have sought to develop nodal methods which have sound theoretical basis and which converge to the correct solution as the node sizes are taken smaller. The transverse integrated nodal method is based on integrating the three (or two) dimensional diffusion equation over the transverse direction(s) and reducing it to a one dimensional diffusion equation, with transverse leakage terms. The most popular of the transverse integrated nodal methods is based on a polynomial expansion of the one dimensional flux and can obtain higher orders of accuracy than conventional finite difference methods [4].

1.4 Finite Element Method

The finite element method (FEM) provides a systematic approach for developing solutions with higher order accuracy than the conventional finite difference equations. Although FEM could be based on a weighed residual approach, FEM applications to the neutron diffusion depend usually on the equivalence of the solution of the diffusion equation with the minimization of a functional. System of interest is divided into homogeneous regions of specified geometric shape which are called finite elements. The spatial dependence of the neutron flux (and sometimes current) is assumed to be a polynomial of a certain degree within the element. The degree of the polynomial dependence determines the name of a particular FEM application (i.e. linear, quadratic, cubic etc. finite elements) [4].

FEM is a coarse-mesh method. Like nodal methods, coarse-mesh methods generally require detailed regional heterogeneous flux distributions in order to construct homogenized parameters and to combine with the coarse-mesh solution to construct a detailed heterogeneous flux solution [2].

1.5 Objectives of the Work

The objective of this thesis is to develop a nodal method which gives acceptably accurate results for realistic problems at a considerable savings over finite difference methods. This method is capable of calculating multiregional and multigroup problems in a one dimensional cylindrical geometry. Comparison this method with FEM is another aim of this work. These are accomplished by using a computer program written in FORTRAN 90. It is named NEMR as the abbreviation of nodal expansion method in r dimension for the cylinder.

Chapter 2 is about the development of a transverse integrated nodal method. A nodal formalism is obtained using lowest order nodal expansion method. The expansion coefficients are determined by applying Fick's law in combination with continuity of normal current. Three equations for each node are obtained. Nodal balance equation constitutes one equation and other two equations are derived from Fick's law. These equations are used to form a matrix equation. Then, a computer program which can carry out criticality-eigenvalue calculations in multigroup diffusion theory is developed using this matrix form. This program can find effective multiplication

factor, flux and current distribution and average fluxes for multigroup and multiregion problems.

Chapter 3 is devoted to validation of this program. It is run for the problems which have been solved analytically. Results are compared with analytical and FEM solutions. Linear and quadratic finite element method results are obtained using a FORTRAN 90 program called QFEMR. (Quadratic Finite Element Method in R dimension)

Chapter 4 includes the conclusion and recommendations for future work.

Finally, appendixes are given for the description of NEMR program.

2 NODAL FORMALISM IN CYLINDRICAL GEOMETRY

2.1 Cell and Edge Averaged Quantities

The multigroup neutron balance equation

$$\vec{\nabla}\cdot\vec{J}_g(\vec{r})+\Sigma_r^g(\vec{r})\phi_g(\vec{r})=\sum_{g'=1}^{g-1}\Sigma^{g'\to g}(\vec{r})\phi_{g'}(\vec{r})+\frac{\chi^g}{k}\sum_{g'=1}^{G}\upsilon\Sigma_f^{g'}(\vec{r})\phi_{g'}(\vec{r}),\ g=1,2,\cdots,G \tag{2.1}$$

with no group-to-group upscatter assumption, and Fick's Law

$$\vec{J}_g(\vec{r})=-D^g(\vec{r})\vec{\nabla}\phi_g(\vec{r}) \tag{2.2}$$

constitute the basis of the nodal formalism.

To avoid complexity in notation, scattering and fission sources will be defined as

$$Q_g(\vec{r})=\sum_{g'=1}^{g-1}\Sigma^{g'\to g}(\vec{r})\phi_{g'}(\vec{r})+\frac{\chi^g}{k}\sum_{g'=1}^{G}\upsilon\Sigma_f^{g'}(\vec{r})\phi_{g'}(\vec{r}),\ g=1,2,\cdots,G \tag{2.3}$$

Thus, (2.1) becomes

$$\vec{\nabla}\cdot\vec{J}_g(\vec{r})+\Sigma_r^g(\vec{r})\phi_g(\vec{r})=Q_g(\vec{r}) \tag{2.4}$$

Since group index is of no immediate concern in nodal development, the group indices will be suppressed and (2.4) and (2.2) will be written as

$$\vec{\nabla}\cdot\vec{J}(\vec{r})+\Sigma_r(\vec{r})\phi(\vec{r})=Q(\vec{r}) \tag{2.5}$$

$$\vec{J}(\vec{r})=-D(\vec{r})\vec{\nabla}\phi(\vec{r}) \tag{2.6}$$

Although nodal methods are generally devised for three dimensional whole core calculations, the transverse integration procedure fails in (r,θ) or (r,θ,z) cylindrical geometry. Because the transverse integration over r (in 2-d) or z and r (in 3-d) leads to an impasse. The difficulty arises with the azimuthal term [5]. This impasse may be circumvented using analytical methods but it is not within the scope of this work. Here a one dimensional development is presented. However, extension from 1-d (r) to 2-d (r-z) is actually trivial for further studies.

Figure 2.1 illustrates a cylindrical mesh having nodes $A_i=(r_{i-1/2}, r_{i+1/2})$. The radii at node centers are similarly denoted as (r_i) and it is convenient to define mesh spacing $\Delta r_i=r_{i+1/2}-r_{i-1/2}$.

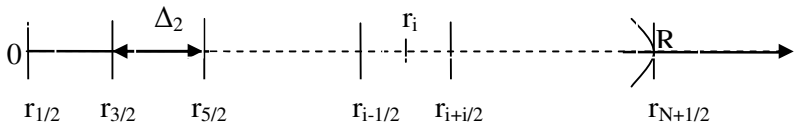

Figure 2.1 Nodal Mesh Imposed on One-dimensional Cylindrical Domain

Δr_i is replaced with Δ_i for simplicity

$$\Delta_i = r_{i+1/2} - r_{i-1/2} \tag{2.7}$$

Inherited from the nodal perspective and common to all nodal discretizations is the choice of cell and edge-based unknowns. The cell-based unknowns are defined by

$$\phi_i = \frac{2}{(r_{i+1/2}^2 - r_{i-1/2}^2)} \int_{r_{i-1/2}}^{r_{i+1/2}} \phi(r) r dr \tag{2.8}$$

$$Q_i = \frac{2}{(r_{i+1/2}^2 - r_{i-1/2}^2)} \int_{r=r_{i-1/2}}^{r_{i+1/2}} Q(r) r dr \tag{2.9}$$

which are the cell average flux and source. While the edged-based unknowns, namely edge average fluxes and currents are just point fluxes and currents at node boundaries in one dimension, because there is no other dimension over which to find averages. They are shown as $\phi_{i+1/2}$, $\phi_{i-1/2}$ and $J_{i+1/2}$, $J_{i-1/2}$

In some nodal methods, edge-averaged partial currents are also needed. To avoid notational complexity, the partial currents will be denoted by the lower case letter j. $j_{i+1/2}^+$ and $j_{i-1/2}^-$ denote the outgoing partial currents, while $j_{i+1/2}^-$ and $j_{i-1/2}^+$ are the incoming partial currents at the right (i+1/2) and left (i-1/2) edges respectively.

Under P_1 approximation

$$j_u^{\pm}(r) = \frac{\phi(r)}{4} \pm \frac{\vec{n}_u \cdot \vec{J}(r)}{2} \tag{2.10}$$

where u is an arbitrary direction.

If diffusion theory is valid,

$$j_u^{\pm}(r) = \frac{1}{4}\phi(r) \mp \frac{D(r)}{2}\frac{\partial \phi}{\partial u}(r) \tag{2.11}$$

from (2.10), obviously:

$$J_{i+1/2} = j^{+}_{i+1/2} - j^{-}_{i+1/2} \tag{2.12}$$

$$J_{i-1/2} = j^{+}_{i-1/2} - j^{-}_{i-1/2} \tag{2.13}$$

and

$$\phi_{i+1/2} = 2\left(j^{+}_{i+1/2} + j^{-}_{i+1/2}\right) \tag{2.14}$$

$$\phi_{i-1/2} = 2\left(j^{+}_{i-1/2} + j^{-}_{i-1/2}\right) \tag{2.15}$$

2.2 Nodal Balance Equation

The nodal view of the first order system (2.5) and (2.6) suggests that a natural starting point is to integrate the exact balance equation (2.5) over an arbitrary cell

$$\int_{V_i} \nabla \cdot J(r)\,dV + \int_{V_i} \Sigma_r(r)\phi(r)\,dV = \int_{V_i} Q(r)\,dV \tag{2.16}$$

In cylindrical coordinates,

$$2\pi \int_{r_{i-1/2}}^{r_{i+1/2}} \frac{1}{r}\frac{d}{dr}\left[rJ(r)\right]rdr + 2\pi\Sigma_r^i \int_{r_{i-1/2}}^{r_{i+1/2}} \phi(r)rdr = 2\pi \int_{r_{i-1/2}}^{r_{i+1/2}} Q(r)rdr \tag{2.17}$$

Since the node is already homogenized, macroscopic removal cross section is constant for a node, $\Sigma_r(r) = \Sigma_r^i$ and it is also assumed constant for all nodes of the same material, $\Sigma_r^i = \Sigma_r$. When the integrations are carried out with the help of (2.8) and (2.9), (2.17) becomes:

$$2\pi\left[r_{i+1/2}J_{i+1/2} - r_{i-1/2}J_{i-1/2}\right] + \frac{\Sigma_r\phi_i\, 2\pi(r_{i+1/2}^2 - r_{i-1/2}^2)}{2} = \frac{Q_i\, 2\pi(r_{i+1/2}^2 - r_{i-1/2}^2)}{2} \tag{2.18}$$

where ϕ_i and Q_i represent the node averaged flux and source respectively.

Surface areas can be defined as

$$S_{i+1/2} = 2\pi r_{i+1/2}, \text{ and } \quad S_{i-1/2} = 2\pi r_{i-1/2} \tag{2.19}$$

Combining (2.7) and (2.19) with (2.18) gives

$$S_{i+1/2}J_{i+1/2} - S_{i-1/2}J_{i-1/2} + \frac{\Sigma_r \Phi_i \Delta_i}{2}\left(S_{i+1/2} + S_{i-1/2}\right) = \frac{Q_i \Delta_i}{2}\left(S_{i+1/2} + S_{i-1/2}\right) \tag{2.20}$$

Surface areas at nodes are

$$S_i = 2\pi r_i \tag{2.21}$$

where r_i can be written as

$$r_i = \frac{r_{i+1/2} + r_{i-1/2}}{2} \tag{2.22}$$

Using (2.21) and (2.22)

$$S_i = \frac{S_{i+1/2} + S_{i-1/2}}{2} \tag{2.23}$$

Substituting (2.13), (2.14) and (2.23) into (2.20), finally, the discrete nodal balance equation is

$$S_{i+1/2}\left(j^+_{i+1/2} - j^-_{i+1/2}\right) - S_{i-1/2}\left(j^+_{i-1/2} - j^-_{i-1/2}\right) + \Sigma_r \Phi_i \Delta_i S_i = Q_i \Delta_i S_i \tag{2.24}$$

Various nodal methods have a common foundation in the discrete nodal balance equation and are characterized by the techniques they employ to derive the additional equations necessary to solve the discrete system.

Two rather distinct classes of nodal methods have evolved. The first class, often referred to as conventional or simulation models, makes use of detailed calculations or reactor operating experience to evaluate the edge averaged currents in terms of differences in cell averaged fluxes for adjacent nodes, with empirically adjusted coupling coefficients. So these methods lack theoretical foundation.

The second class, sometimes referred to as consistently formulated models, makes use of the concept of transverse integration and of higher order (than ordinary finite difference) approximations to evaluate the edge averaged currents and the internodal coupling terms in order to derive nodal equations that can be expected to converge to the exact solution in the limit of small mesh spacing.

2.3 Transverse Integration

Finneman, et al. developed a popular discretization procedure which utilizes the partial current directly. This is transverse integration procedure which has become a cornerstone of modern nodal methods [5].

The usual strategy for solving the neutron diffusion equation in two or three dimensions by nodal methods is to reduce the multidimensional partial differential equation to a set of ordinary differential equations (ODE's) in the separate spatial coordinates. This reduction is accomplished by transverse integration of the equations. In cylindrical coordinates, the three-dimensional equation is first integrated over r and θ to obtain an ODE in z, then over r and z to obtain an ODE in θ, and finally over θ and z to obtain an ODE in r. Then these ODE's are solved to obtain one-dimensional solutions for the neutron fluxes averaged over the other two dimensions. Because the solution in each node is an exact analytical solution, the nodes can be much larger than the mesh elements used in finite-difference solutions. Then the solutions in the different nodes are coupled by applying interface conditions, ultimately fixing the solutions to the external boundary condition [6].

Transverse integrated equations contain transverse leakage terms. They must be satisfied in an integral sense. That is, these equations are multiplied with the weight function and integrated over the node. The integrals of the weighted residue must vanish. This is called as weighted residual procedure. In the lowest order nodal expansion method (NEM), weight function is chosen as one. This procedure gives (2.24), discrete nodal balance equation. In the lowest order case which is treated here, (2.24) is enough to constitute one equation for a node.

There are two distinct applications of the transverse integrated equations. The first is the weighted residual procedure of the NEM by Finneman et al. In one dimensional analysis here, transverse integration is not necessary to reduce dimension. The second variety depends on the analytical solutions of the transverse integrated equations. The second approach has been presented in [6] for cylindrical geometry and in [7]. It will not be treated here.

2.4 Nodal Expansion Method

The development of modern consistent nodal discretizations began in the mid 70's. These methods were based on local polynomial expansions. The first polynomial method was the nodal expansion method (NEM). In fact, although some variations and improvements have been considered, the NEM ideology still dominates the polynomial class of nodal methods.

In this lowest order form, NEM considers a quadratic expansion of the averaged flux on each cell. The expansion coefficients are determined by applying Fick's law in combination with discrete nodal balance equation (2.24) and continuity of normal current.

Considerable effort has been made to utilize higher order polynomial expansion within NEM. The difficulty this creates is centered around the evaluation of the higher order expansion coefficients. In particular, the weighted residual procedure that is typically used relies on transverse-integrated equations and as a result an approximation of the transverse normal currents (i.e. transverse leakage) is also required.

2.4.1 Construction of Polynomial Basis

The NEM treatment of the transverse integrated ODE's is based on a low order polynomial expansion of the transverse integrated flux. In one dimension this is just r dependent flux

$$\phi(r) = \sum_{l=0}^{N} a_l P_l(r), \quad r_{i-1/2} < r < r_{i+1/2} \tag{2.25}$$

At this point a local variable ξ is defined as

$$\xi = \frac{r - r_i}{\Delta_i} \tag{2.26}$$

where $\xi = \pm 1/2$ when $r = r_{i\pm 1/2}$.

ξ and r are the same order. Then, (2.25) can be written in local variable

$$\phi(\xi) = \sum_{l=0}^{N} a_l P_l(\xi), \quad -1/2 < \xi < 1/2 \tag{2.27}$$

where $P_l(\xi)$ is a polynomial of degree *l*.

For simplicity, the first polynomial is chosen as

$$P_0(\xi)=1 \tag{2.28}$$

and the higher order polynomials are required to be orthogonal to $P_0(\xi)$

$$\int_{-1/2}^{1/2} P_l(\xi)\,d\xi = 0, \quad l \neq 0 \tag{2.29}$$

Transformation of integration operator gives

$$d\xi = \frac{dr}{\Delta_i} \tag{2.30}$$

Using (2.30) and (2.26) in (2.8)

$$\phi_i = \frac{2}{(r_{i+1/2}^2 - r_{i-1/2}^2)} \int_{-1/2}^{1/2} \phi(\xi)(\xi\Delta_i + r_i)\Delta_i d\xi \tag{2.31}$$

Substituting (2.22) into (2.31)

$$\phi_i = \frac{1}{\Delta_i r_i} \int_{-1/2}^{1/2} \phi(\xi)(\xi\Delta_i + r_i)\Delta_i d\xi \tag{2.32}$$

Lowest order NEM uses quadratic expansion, so N=2. Inserting (2.27) into (2.32)

$$\phi_i = \frac{1}{\Delta_i r_i} \int_{-1/2}^{1/2} \left(\sum_{l=0}^{N=2} a_l P_l(\xi)\right)(\xi\Delta_i + r_i)\Delta_i d\xi \tag{2.33}$$

Thus

$$\phi_i = \frac{1}{r_i} \int_{-1/2}^{1/2} (a_0 P_0(\xi) + a_1 P_1(\xi) + a_2 P_2(\xi))(\xi\Delta_i + r_i) d\xi \tag{2.34}$$

Using (2.28)

$$\phi_i = \frac{1}{r_i} \int_{-1/2}^{1/2} (a_0\xi\Delta_i + a_1 P_1(\xi)\xi\Delta_i + a_2 P_2(\xi)\xi\Delta_i + a_0 r_i + a_1 P_1(\xi) r_i + a_2 P_2(\xi) r_i) d\xi \tag{2.35}$$

The orthogonality requirement results in last two terms to be vanished in the integrand. Also integration of the first term is zero. Thus

$$\phi_i = \frac{1}{r_i}\left[a_1\Delta_i \int_{-1/2}^{1/2} P_1(\xi)\xi d\xi + a_2\Delta_i \int_{-1/2}^{1/2} P_2(\xi)\xi d\xi + a_0 r_i \int_{-1/2}^{1/2} d\xi \right] \tag{2.36}$$

All odd polynomials satisfy the requirement (2.29). Thus

$$P_1(\xi) = \alpha_1 \xi \tag{2.37}$$

where α_1 is a constant yet to be determined. If an even polynomial has only one term (one monomial), it can never satisfy (2.29), since

$$\int_{-1/2}^{1/2} \xi^n d\xi = \frac{1}{(n+1)2^n}, \quad \text{n even} \tag{2.38}$$

Specifically

$$\int_{-1/2}^{1/2} \xi^2 d\xi = \frac{1}{12} \tag{2.39}$$

Thus any quadratic polynomial of the form

$$P_2(\xi) = \alpha_2\left(\xi^2 - \frac{1}{12}\right) \tag{2.40}$$

would satisfy (2.29).

Substituting (2.37) and (2.40) into (2.36)

$$\phi_i = \frac{1}{r_i}\left[a_1\Delta_i\alpha_1 \int_{-1/2}^{1/2} \xi^2 d\xi + a_2\Delta_i\alpha_2 \int_{-1/2}^{1/2} \xi^3 d\xi - a_2\Delta_i\alpha_2 \int_{-1/2}^{1/2} \frac{\xi}{12} d\xi + a_0 r_i \int_{-1/2}^{1/2} d\xi\right] \tag{2.41}$$

Second and third integrals have to be vanished since they contain odd polynomials

$$\phi_i = \frac{1}{r_i}\left[\frac{a_1\Delta_i\alpha_1}{12} + a_0 r_i\right] = a_0 + \frac{a_1\Delta_i\alpha_1}{12 r_i} \tag{2.42}$$

If ξ=+1/2, this describes node outer boundary

$$\phi_{i+1/2} = \sum_{l=0}^{2} a_l P_l(1/2) = a_0 P_0(1/2) + a_1 P_1(1/2) + a_2 P_2(1/2) \tag{2.43}$$

$$\phi_{i+1/2} = a_0 + a_1\frac{\alpha_1}{2} + a_2\frac{\alpha_2}{6} \tag{2.44}$$

If ξ=-1/2, this describes node inner boundary

$$\phi_{i-1/2} = \sum_{l=0}^{2} a_l P_l(-1/2) = a_0 P_0(-1/2) + a_1 P_1(-1/2) + a_2 P_2(-1/2) \tag{2.45}$$

$$\phi_{i-1/2} = a_0 - a_1\frac{\alpha_1}{2} + a_2\frac{\alpha_2}{6} \tag{2.46}$$

Subtracting (2.46) from (2.44)

$$a_1 = \frac{1}{\alpha_1}\left(\phi_{i+1/2} - \phi_{i-1/2}\right) \tag{2.47}$$

Adding (2.46) and (2.44),

$$\phi_{i+1/2} + \phi_{i-1/2} = 2a_0 + a_2\frac{\alpha_2}{3} \tag{2.48}$$

Substituting (2.47) into (2.42),

$$\phi_i = a_0 + \frac{\Delta_i\left(\phi_{i+1/2} - \phi_{i-1/2}\right)}{12r_i} \tag{2.49}$$

Thus

$$a_0 = \phi_i + \frac{\Delta_i\phi_{i-1/2}}{12r_i} - \frac{\Delta_i\phi_{i+1/2}}{12r_i} \tag{2.50}$$

Substituting (2.50) into (2.48),

$$\phi_{i+1/2} + \phi_{i-1/2} = 2\phi_i + \frac{\Delta_i\phi_{i-1/2}}{6r_i} - \frac{\Delta_i\phi_{i+1/2}}{6r_i} + a_2\frac{\alpha_2}{3} \tag{2.51}$$

The last coefficient a_2 is found from (2.51)

$$a_2 = \frac{3}{\alpha_2}\left(\left(\frac{6r_i + \Delta_i}{6r_i}\right)\phi_{i+1/2} - 2\phi_i + \left(\frac{6r_i - \Delta_i}{6r_i}\right)\phi_{i-1/2}\right) \tag{2.52}$$

To make (2.47) and (2.52) as simple as possible, α_1=1 and α_2=3 are chosen. Polynomial basis are constructed for the lowest order NEM as

$$P_1(\xi) = \xi \tag{2.53}$$

$$P_2(\xi) = 3\xi^2 - \frac{1}{4} \tag{2.54}$$

Using these polynomials and coefficients in (2.27),

$$\begin{aligned}\phi(\xi) = &\left[\phi_i + \frac{\Delta_i\phi_{i-1/2}}{12r_i} - \frac{\Delta_i\phi_{i+1/2}}{12r_i}\right]1 + \left[\left(\phi_{i+1/2} - \phi_{i-1/2}\right)\right]\xi \\ &+ \left[\left(\frac{6r_i + \Delta_i}{6r_i}\right)\phi_{i+1/2} - 2\phi_i + \left(\frac{6r_i - \Delta_i}{6r_i}\right)\phi_{i-1/2}\right]\left(3\xi^2 - \frac{1}{4}\right)\end{aligned} \tag{2.55}$$

Finally, after some arrangements in (2.55)

$$\phi(\xi) = \left(\frac{3}{2} - 6\xi^2\right)\phi_i + \left(\frac{-1}{8(r_i/\Delta_i)} - \frac{1}{4} + \xi + \left(3 + \frac{1}{2(r_i/\Delta_i)}\right)\xi^2\right)\phi_{i+1/2} + \left(\frac{1}{8(r_i/\Delta_i)} - \frac{1}{4} - \xi + \left(3 - \frac{1}{2(r_i/\Delta_i)}\right)\xi^2\right)\phi_{i-1/2} \quad (2.56)$$

2.4.2 Fick's Law

Fick's law states that

$$J(r) = -D\frac{d\phi(r)}{dr} \quad (2.57)$$

Note that

$$\frac{d\phi(r)}{dr} = \frac{d\phi}{d\xi}\frac{d\xi}{dr} = \frac{1}{\Delta_i}\frac{d\phi(r)}{d\xi} \quad (2.58)$$

(2.57) may be written as

$$J(\xi) = -\frac{D_i}{\Delta_i}\frac{d\phi(\xi)}{d\xi} \quad (2.59)$$

Using (2.56)

$$\frac{d\phi(\xi)}{d\xi} = -12\xi\phi_i + \left(1 + 2\xi\left(3 + \frac{1}{2(r_i/\Delta_i)}\right)\right)\phi_{i+1/2} + \left(-1 + 2\xi\left(3 - \frac{1}{2(r_i/\Delta_i)}\right)\right)\phi_{i-1/2} \quad (2.60)$$

Substituting (2.60) into (2.59), for ξ=+1/2

$$J_{i+1/2} = -\frac{D_i}{\Delta_i}\left(-6\phi_i + \left(4 + \frac{1}{2(r_i/\Delta_i)}\right)\phi_{i+1/2} + \left(2 - \frac{1}{2(r_i/\Delta_i)}\right)\phi_{i-1/2}\right) \quad (2.61)$$

Similarly, for ξ=-1/2

$$J_{i-1/2} = -\frac{D_i}{\Delta_i}\left(6\phi_i - \left(2 + \frac{1}{2(r_i/\Delta_i)}\right)\phi_{i+1/2} - \left(4 - \frac{1}{2(r_i/\Delta_i)}\right)\phi_{i-1/2}\right) \quad (2.62)$$

(2.61) may be written in terms of edge averaged partial currents, using (2.14) and (2.15)

$$J_{i+1/2} = \frac{6D_i\phi_i}{\Delta_i} - \frac{2D_i}{\Delta_i}\left(4 + \frac{1}{2(r_i/\Delta_i)}\right)\left[j^+_{i+1/2} + j^-_{i+1/2}\right]$$
$$- \frac{2D_i}{\Delta_i}\left(2 - \frac{1}{2(r_i/\Delta_i)}\right)\left[j^+_{i-1/2} + j^-_{i-1/2}\right] \tag{2.63}$$

Using (2.12) in (2.63) and after arrangements

$$\left(1 + \frac{8D_i}{\Delta_i} + \frac{D_i}{r_i}\right)j^+_{i+1/2} = \left(1 - \frac{8D_i}{\Delta_i} - \frac{D_i}{r_i}\right)j^-_{i+1/2} - \left(\frac{4D_i}{\Delta_i} - \frac{D_i}{r_i}\right)j^+_{i-1/2}$$
$$- \left(\frac{4D_i}{\Delta_i} - \frac{D_i}{r_i}\right)j^-_{i-1/2} + \frac{6D_i}{\Delta_i}\phi_i \tag{2.64}$$

Similarly, using (2.13), (2.14), and (2.15), in (2.62)

$$j^+_{i-1/2} - j^-_{i-1/2} = -\frac{6D_i}{\Delta_i}\phi_i + \frac{2D_i}{\Delta_i}\left(2 + \frac{1}{2(r_i/\Delta_i)}\right)j^+_{i+1/2} + \frac{2D_i}{\Delta_i}\left(2 + \frac{1}{2(r_i/\Delta_i)}\right)j^-_{i+1/2}$$
$$+ \frac{2D_i}{\Delta_i}\left(4 - \frac{1}{2(r_i/\Delta_i)}\right)j^+_{i-1/2} + \frac{2D_i}{\Delta_i}\left(4 - \frac{1}{2(r_i/\Delta_i)}\right)j^-_{i-1/2} \tag{2.65}$$

After some arrangements

$$-\left(1 + \frac{8D_i}{\Delta_i} - \frac{D_i}{r_i}\right)j^-_{i-1/2} = \left(\frac{4D_i}{\Delta_i} + \frac{D_i}{r_i}\right)j^+_{i+1/2} + \left(\frac{4D_i}{\Delta_i} + \frac{D_i}{r_i}\right)j^-_{i+1/2}$$
$$-\left(1 - \frac{8D_i}{\Delta_i} + \frac{D_i}{r_i}\right)j^+_{i-1/2} - \frac{6D_i}{\Delta_i}\phi_i \tag{2.66}$$

(2.64) and (2.66) are the expressions for the outgoing partial currents. Substituting the outgoing current $j^-_{i-1/2}$ defined by (2.66) into (2.64) gives

$$\left(1+\frac{8D_i}{\Delta_i}+\frac{D_i}{r_i}\right)j^+_{i+1/2}=\left(1-\frac{8D_i}{\Delta_i}-\frac{D_i}{r_i}\right)j^-_{i+1/2}-\left(\frac{4D_i}{\Delta_i}-\frac{D_i}{r_i}\right)j^+_{i-1/2}$$

$$+\frac{\left(\frac{4D_i}{\Delta_i}-\frac{D_i}{r_i}\right)\left(\frac{4D_i}{\Delta_i}+\frac{D_i}{r_i}\right)}{\left(1+\frac{8D_i}{\Delta_i}-\frac{D_i}{r_i}\right)}j^+_{i+1/2}+\frac{\left(\frac{4D_i}{\Delta_i}-\frac{D_i}{r_i}\right)\left(\frac{4D_i}{\Delta_i}+\frac{D_i}{r_i}\right)}{\left(1+\frac{8D_i}{\Delta_i}-\frac{D_i}{r_i}\right)}j^-_{i+1/2} \tag{2.67}$$

$$-\frac{\left(\frac{4D_i}{\Delta_i}-\frac{D_i}{r_i}\right)\left(1-\frac{8D_i}{\Delta_i}+\frac{D_i}{r_i}\right)}{\left(1+\frac{8D_i}{\Delta_i}-\frac{D_i}{r_i}\right)}j^+_{i-1/2}-\frac{\left(\frac{4D_i}{\Delta_i}-\frac{D_i}{r_i}\right)6D_i\phi_i}{\Delta_i\left(1+\frac{8D_i}{\Delta_i}-\frac{D_i}{r_i}\right)}+\frac{6D_i}{\Delta_i}\phi_i$$

Collecting terms

$$j^+_{i+1/2}\left[\left(1+\frac{8D_i}{\Delta_i}+\frac{D_i}{r_i}\right)-\frac{\frac{16D_i^2}{\Delta_i^2}-\frac{D_i^2}{r_i^2}}{\left(1+\frac{8D_i}{\Delta_i}+\frac{D_i}{r_i}\right)}\right]=$$

$$-j^+_{i-1/2}\left[\frac{4D_i}{\Delta_i}-\frac{D_i}{r_i}+\frac{\left(\frac{4D_i}{\Delta_i}-\frac{D_i}{r_i}\right)\left(1-\frac{8D_i}{\Delta_i}+\frac{D_i}{r_i}\right)}{\left(1+\frac{8D_i}{\Delta_i}-\frac{D_i}{r_i}\right)}\right] \tag{2.68}$$

$$+j^-_{i+1/2}\left[\left(1-\frac{8D_i}{\Delta_i}-\frac{D_i}{r_i}\right)+\frac{\frac{16D_i^2}{\Delta_i^2}-\frac{D_i^2}{r_i^2}}{\left(1+\frac{8D_i}{\Delta_i}-\frac{D_i}{r_i}\right)}\right]+\phi_i\left[\frac{6D_i}{\Delta_i}-\frac{6D_i\left(\frac{4D_i}{\Delta_i}-\frac{D_i}{r_i}\right)}{\Delta_i\left(1+\frac{8D_i}{\Delta_i}-\frac{D_i}{r_i}\right)}\right]$$

Simplifying (2.68) yields

$$j^+_{i+1/2}\left[1+\frac{16D_i}{\Delta_i}+\frac{48D_i^2}{\Delta_i^2}\right]=j^+_{i-1/2}\left[\frac{2D_i}{r_i}-\frac{8D_i}{\Delta_i}\right]$$

$$+j^-_{i+1/2}\left[1-\frac{2D_i}{r_i}-\frac{48D_i^2}{\Delta_i^2}\right]+\phi_i\left[\frac{6D_i}{\Delta_i}+\frac{24D_i^2}{\Delta_i^2}\right] \tag{2.69}$$

Similarly, substituting the outgoing current $j^+_{i+1/2}$ defined by (2.64) into (2.66)

$$-\left(1+\frac{8D_i}{\Delta_i}-\frac{D_i}{r_i}\right)j^-_{i-1/2}=\frac{\left(\frac{4D_i}{\Delta_i}+\frac{D_i}{r_i}\right)\left(1-\frac{8D_i}{\Delta_i}-\frac{D_i}{r_i}\right)}{\left(1+\frac{8D_i}{\Delta_i}+\frac{D_i}{r_i}\right)}j^-_{i+1/2}$$

$$-\frac{\left(\frac{16D_i^2}{\Delta_i^2}-\frac{D_i^2}{r_i^2}\right)}{\left(1+\frac{8D_i}{\Delta_i}+\frac{D_i}{r_i}\right)}j^+_{i-1/2}-\frac{\left(\frac{16D_i^2}{\Delta_i^2}-\frac{D_i^2}{r_i^2}\right)}{\left(1+\frac{8D_i}{\Delta_i}+\frac{D_i}{r_i}\right)}j^-_{i-1/2}+\frac{\left(\frac{4D_i}{\Delta_i}+\frac{D_i}{r_i}\right)\frac{6D_i}{\Delta_i}}{\left(1+\frac{8D_i}{\Delta_i}+\frac{D_i}{r_i}\right)}\phi_i \tag{2.70}$$

$$+\left(\frac{4D_i}{\Delta_i}+\frac{D_i}{r_i}\right)j^-_{i+1/2}-\left(1-\frac{8D_i}{\Delta_i}+\frac{D_i}{r_i}\right)j^+_{i-1/2}+\frac{6D_i}{\Delta_i}\phi_i$$

Collecting terms in (2.70)

$$j^-_{i-1/2}\left[\frac{\left(\frac{16D_i^2}{\Delta_i^2}-\frac{D_i^2}{r_i^2}\right)-\left(1+\frac{8D_i}{\Delta_i}-\frac{D_i}{r_i}\right)\left(1+\frac{8D_i}{\Delta_i}+\frac{D_i}{r_i}\right)}{\left(1+\frac{8D_i}{\Delta_i}+\frac{D_i}{r_i}\right)}\right]=$$

$$j^-_{i+1/2}\left[2\frac{\left(\frac{4D_i}{\Delta_i}+\frac{D_i}{r_i}\right)}{\left(1+\frac{8D_i}{\Delta_i}+\frac{D_i}{r_i}\right)}\right]-j^+_{i-1/2}\left[\frac{\left(1-\frac{8D_i}{\Delta_i}+\frac{D_i}{r_i}\right)\left(1+\frac{8D_i}{\Delta_i}+\frac{D_i}{r_i}\right)+\frac{16D_i^2}{\Delta_i^2}-\frac{D_i^2}{r_i^2}}{\left(1+\frac{8D_i}{\Delta_i}+\frac{D_i}{r_i}\right)}\right] \tag{2.71}$$

$$+\phi_i\left[\frac{\frac{6D_i}{\Delta_i}\left(-\frac{4D_i}{\Delta_i}-1\right)}{\left(1+\frac{8D_i}{\Delta_i}+\frac{D_i}{r_i}\right)}\right]$$

Simplifying (2.71)

$$j^-_{i-1/2}\left[1+\frac{16D_i}{\Delta_i}+\frac{48D_i^2}{\Delta_i^2}\right]=j^-_{i+1/2}\left[-\frac{2D_i}{r_i}-\frac{8D_i}{\Delta_i}\right]$$

$$+j^+_{i-1/2}\left[1+\frac{2D_i}{r_i}-\frac{48D_i^2}{\Delta_i^2}\right]+\phi_i\left[\frac{6D_i}{\Delta_i}+\frac{24D_i^2}{\Delta_i^2}\right] \tag{2.72}$$

If a dimensionless variable is defined as

$$\tau_i = \left(1 + \frac{16D_i}{\Delta_i} + \frac{48D_i^2}{\Delta_i^2}\right) \tag{2.73}$$

(2.69) becomes

$$j^+_{i+1/2} = \frac{2D_i\left(\frac{1}{r_i} - \frac{4}{\Delta_i}\right)}{\tau_i} j^+_{i-1/2} + \frac{\left(1 - \frac{2D_i}{r_i} - \frac{48D_i^2}{\Delta_i^2}\right)}{\tau_i} j^-_{i+1/2} + \frac{\frac{6D_i}{\Delta_i}\left(1 + \frac{4D_i}{\Delta_i}\right)}{\tau_i}\phi_i \tag{2.74}$$

and (2.72) becomes

$$j^-_{i-1/2} = \frac{-2D_i\left(\frac{1}{r_i} + \frac{4}{\Delta_i}\right)}{\tau_i} j^-_{i+1/2} + \frac{\left(1 + \frac{2D_i}{r_i} - \frac{48D_i^2}{\Delta_i^2}\right)}{\tau_i} j^+_{i-1/2} + \frac{6D_i}{\Delta_i\tau_i}\left(1 + \frac{4D_i}{\Delta_i}\right)\phi_i \tag{2.75}$$

(2.74) and (2.75) constitute 2 equations per node. The number of unknowns per node is three. The outgoing partial currents ($j^+_{i+1/2}, j^-_{i-1/2}$) and the cell flux ϕ_i constitute the three unknowns. The incoming partial currents ($j^+_{i-1/2}, j^-_{i+1/2}$) can be considered known quantities, since they are either equal to the outgoing partial currents of the neighboring cells or are known from boundary condition.

The remarks above are valid if conventional homogenization theory is used and, thus continuity of partial currents is assumed. If equivalence homogenization theory is used; the incoming partial currents are not equal to the outgoing partial currents of the neighboring cells. The incoming partial current can be written in terms of the outgoing partial current of the neighboring cell, outgoing partial current of the same cell and the flux discontinuity factors.

If we wish to use a higher order flux expansion, say N=4, the higher order flux moments appear in their counterpart of the two equations (2.74) and (2.75). Thus, extra equations are needed. Weighted residual procedure equates the number of unknowns to the number of equations provided the treatment of transverse leakage term does not introduce any extra unknowns. The most successful approximation for the treatment of the transverse leakage term has been an approximation called quadratic approximation [8].

2.5 Iterative Solution of the Nodal Equations

(2.74) and (2.75) can be written in shorter forms, if the following variables are defined

$$m_i = \frac{2D_i\left(\frac{1}{r_i} - \frac{4}{\Delta_i}\right)}{\tau_i} \tag{2.76}$$

$$n_i = \frac{\left(1 - \frac{2D_i}{r_i} - \frac{48D_i^2}{\Delta_i^2}\right)}{\tau_i} \tag{2.77}$$

$$p_i = \frac{\frac{6D_i}{\Delta_i}\left(1 + \frac{4D_i}{\Delta_i}\right)}{\tau_i} \tag{2.78}$$

$$o_i = \frac{\left(1 + \frac{2D_i}{r_i} - \frac{48D_i^2}{\Delta_i^2}\right)}{\tau_i} \tag{2.79}$$

$$t_i = \frac{-2D_i\left(\frac{1}{r_i} + \frac{4}{\Delta_i}\right)}{\tau_i} \tag{2.80}$$

Therefore (2.75) becomes

$$j^+_{i+1/2} = m_i j^+_{i-1/2} + n_i j^-_{i+1/2} + p_i \phi_i \tag{2.81}$$

$$j^-_{i-1/2} = t_i j^-_{i+1/2} + o_i j^+_{i-1/2} + p_i \phi_i \tag{2.82}$$

Here $J^-_{i+1/2}$ and $j^+_{i-1/2}$ are known quantities. But $j^+_{i+1/2}$, $j^-_{i-1/2}$ and ϕ_i are unknowns. So a third equation is necessary for the determination of the three nodal unknowns. It's the discrete nodal balance equation. From (2.24)

$$\phi_i = -\frac{\left[S_{i+1/2}\left(j^+_{i+1/2} - j^-_{i+1/2}\right) - S_{i-1/2}\left(j^+_{i-1/2} - j^-_{i-1/2}\right)\right]}{\Sigma_r \Delta_i S_i} + \frac{Q_i \Delta_i S_i}{\Sigma_r \Delta_i S_i} \tag{2.83}$$

(2.83) can be written as

$$\phi_i = \frac{1}{\Sigma_r}\left[Q_i - \frac{1}{\Delta_i S_i}\left[\left(S_{i+1/2} j^+_{i+1/2} + S_{i-1/2} j^-_{i-1/2}\right) - \left(S_{i+1/2} j^-_{i+1/2} + S_{i-1/2} j^+_{i-1/2}\right)\right]\right] \tag{2.84}$$

2.5.1 Matrix Equation

(2.81) and (2.82) can be put into matrix form as

$$\begin{bmatrix} j^{+}_{i+1/2} \\ j^{-}_{i-1/2} \end{bmatrix} = \begin{bmatrix} m_i & n_i \\ o_i & t_i \end{bmatrix} \begin{bmatrix} j^{+}_{i-1/2} \\ j^{-}_{i+1/2} \end{bmatrix} + \phi_i \begin{bmatrix} p_i \\ p_i \end{bmatrix} \tag{2.85}$$

(2.85) can be written shortly

$$\underline{j}^{out} = \underline{\underline{R}}\,\underline{j}^{in} + \phi_i \underline{p} \tag{2.86}$$

and (2.84) can be written as

$$\phi_i = \frac{1}{\Sigma_r}\left[Q_i - \underline{S}^T\left(\underline{j}^{out} - \underline{j}^{in}\right)\right] \tag{2.87}$$

where

$$\underline{S}^T = \frac{1}{\Delta_i S_i}\left[S_{i+1/2} \;\; S_{i-1/2}\right] \tag{2.88}$$

$$\underline{\underline{R}} = \begin{bmatrix} m_i & n_i \\ o_i & t_i \end{bmatrix} \tag{2.89}$$

$$\underline{j}^{out} = \begin{bmatrix} j^{+}_{i+1/2} \\ j^{-}_{i-1/2} \end{bmatrix} \quad \text{and} \quad \underline{j}^{in} = \begin{bmatrix} j^{+}_{i-1/2} \\ j^{-}_{i+1/2} \end{bmatrix} \tag{2.90}$$

(2.86) and (2.87) are used for iterative process. One method is to use two matrix equations separately. Q_i would be known from estimates k_{eff} and ϕ_i of the previous outer iteration or initial guess. Inner iteration provides estimates of the incoming partial currents and cell average fluxes. A marching procedure takes places throughout the core in an inner iteration. Inner iteration ends when the per cent difference between the consecutive estimates of the cell averaged fluxes drops below a certain predetermined convergence criteria.

After the convergence of the inner iteration, next outer iteration begins and a new k_{eff} estimate is found. The outer iterations stop when the percent error between k_{eff} estimates drops a certain predetermined convergence criterion.

Alternatively, (2.86) and (2.87) are written in one matrix equation form as

$$\underline{\underline{A}}\underline{J} = \frac{1}{k_{eff}}\,\underline{\underline{F}}\,\underline{J} + \underline{S} \tag{2.91}$$

Here, $\underline{J}$ is the unknown vector. It contains outgoing partial currents and cell average fluxes. $\underline{\underline{A}}$ is 3Nx3N band matrix, where N is the total number of nodes. $\underline{\underline{F}}$ is again 3Nx3N diagonal matrix and only (3i-1)th elements contain nonzero fission source term. (i=1,2,…N) $\underline{S}$ is the scattering source vector. In the first iteration, right hand side (RHS) of (2.91) is known. $\underline{J}$ is known from initial estimates of outgoing partial currents and cell averaged fluxes.

$$\underline{\underline{A}}\underline{J}^{(n+1)} = \underline{b}^{(n)} \tag{2.92}$$

New $\underline{J}$ vector is found with a linear system solver which has two main subroutines, first makes LU factorization of the matrix $\underline{\underline{A}}$ and second solves the system. New k_{eff} estimate is found after fission source iteration. Iteration continues until the difference between two successive k_{eff} estimates drops below the convergence criterion. Converged $\underline{J}$ vector contains both fluxes and currents as it is shown in (2.93) and they are separated into flux and current vectors in the next step.

$$\underline{J}^T = \left[j^-_{1/2} \quad \phi_1 \quad j^+_{3/2} \quad j^-_{3/2} \quad \phi_2 \quad j^+_{5/2} \cdots\cdots\cdots\cdots j^-_{(2N-1)/2} \quad \phi_N \quad j^+_{(2N+1)/2} \right] \tag{2.93}$$

2.5.2 One-Node Formulation

In one-group formulation, removal cross section is equal to the absorption cross section. Node thickness is equal to the radius of the cylinder. Only fission source exists.

Then, (2.82), (2.84) and (2.81) become

$$j^-_{1/2} = t_1 j^-_{3/2} + o_1 j^+_{1/2} + p_1 \phi_1 \tag{2.94}$$

$$\phi_1 = \frac{\nu\Sigma_f}{\Sigma_a k_{eff}}\phi_1 - \frac{S_{3/2} j^+_{3/2}}{\Sigma_a \Delta S_1} - \frac{S_{1/2} j^-_{1/2}}{\Sigma_a \Delta S_1} + \frac{S_{3/2} j^-_{3/2}}{\Sigma_a \Delta S_1} + \frac{S_{1/2} j^+_{1/2}}{\Sigma_a \Delta S_1} \tag{2.95}$$

$$j^+_{3/2} = m_1 j^+_{1/2} + n_1 j^-_{3/2} + p_1 \phi_1 \tag{2.96}$$

Boundary conditions are $J_{1/2} = j^+_{1/2} - j^-_{1/2} = 0 \rightarrow j^+_{1/2} = j^-_{1/2}$ (reflective) and $j^-_{3/2} = 0$ (vacuum). Also $S_{1/2}$=0, no surface area exists at the center of the cylinder. Thus, after the application of boundary conditions, the equations (2.94), (2.95) and (2.96) describe the whole system:

$$(1 - o_1) j^+_{1/2} - p_1 \phi_1 = 0 \tag{2.97}$$

$$\phi_1 + \frac{S_{3/2} j^+_{3/2}}{\Sigma_a \Delta S_1} = \frac{\nu \Sigma_f}{\Sigma_a k_{eff}} \tag{2.98}$$

$$j^+_{3/2} - m_1 j^+_{1/2} - p_1 \phi_1 = 0 \tag{2.99}$$

In matricial form

$$\underline{\underline{A}}_1 \underline{J}_1 = \frac{1}{k_{eff}} \underline{\underline{F}}_1 \underline{J}_1 \tag{2.100}$$

where

$$\underline{\underline{A}}_1 = \begin{bmatrix} 1 - o_1 & -p_1 & 0 \\ 0 & 1 & \frac{S_{3/2}}{\Sigma_a \Delta S_1} \\ -m_1 & -p_1 & 1 \end{bmatrix} \tag{2.101}$$

$$\underline{J}_1^T = \begin{bmatrix} j^+_{1/2} & \phi_1 & j^+_{3/2} \end{bmatrix} \tag{2.102}$$

$$\underline{\underline{F}}_1 = \begin{bmatrix} 0 & 0 & 0 \\ 0 & \frac{\nu \Sigma_f}{\Sigma_a} & 0 \\ 0 & 0 & 0 \end{bmatrix} \tag{2.103}$$

2.5.3 Two-Node Formulation

Whole system is homogeneous and the nodes have equal thickness. If i=1,

$$(1 - o_1) j^+_{1/2} - p_1 \phi_1 - t_1 j^-_{3/2} = 0 \tag{2.104}$$

$$\phi_1 + \frac{S_{3/2} j^+_{3/2}}{\Sigma_a \Delta S_1} - \frac{S_{3/2} j^-_{3/2}}{\Sigma_a \Delta S_1} = \frac{\nu \Sigma_f}{\Sigma_a k_{eff}} \phi_1 \tag{2.105}$$

$$j^+_{3/2} - m_1 j^+_{1/2} - n_1 J^-_{3/2} - p_1 \phi_1 = 0 \tag{2.106}$$

For i=2, $j^-_{5/2} = 0$ (boundary condition)

$$j^-_{3/2} - o_2 j^+_{3/2} - p_2 \phi_2 = 0 \tag{2.107}$$

$$\phi_2 + \frac{S_{5/2} j^+_{5/2}}{\Sigma_a \Delta S_2} + \frac{S_{3/2} j^-_{3/2}}{\Sigma_a \Delta S_2} - \frac{S_{3/2} j^+_{3/2}}{\Sigma_a \Delta S_2} = \frac{\nu \Sigma_f}{\Sigma_a k_{eff}} \phi_2 \tag{2.108}$$

$$j^+_{5/2} - m_2 j^+_{3/2} - p_2 \phi_2 = 0 \tag{2.109}$$

(2.104) through (2.109) can be written in matrix form

$$\underline{\underline{A}}_2 \underline{J}_2 = \frac{1}{k_{eff}} \underline{\underline{F}}_2 \underline{J}_2 \qquad (2.110)$$

where

$$\underline{\underline{A}}_2 = \begin{bmatrix} & & & -t_1 & 0 & 0 \\ & \underline{\underline{A}}_1^{(3x3)} & & -\frac{S_{3/2}}{\Sigma_a \Delta S_1} & 0 & 0 \\ & & & -n_1 & 0 & 0 \\ 0 & 0 & -o_2 & 1 & -p_2 & 0 \\ 0 & 0 & -\frac{S_{3/2}}{\Sigma_a \Delta S_2} & \frac{S_{3/2}}{\Sigma_a \Delta S_2} & 1 & \frac{S_{5/2}}{\Sigma_a \Delta S_2} \\ 0 & 0 & -m_2 & 0 & -p_2 & 1 \end{bmatrix}_{6x6} \qquad (2.111)$$

$$\underline{J}_2^T = \left[j_{1/2}^+ \quad \phi_1 \quad j_{3/2}^+ \quad j_{3/2}^- \quad \phi_2 \quad j_{5/2}^+ \right] \qquad (2.112)$$

$$\underline{\underline{F}}_2 = \begin{bmatrix} \underline{\underline{F}}_1^{(3x3)} & \underline{\underline{0}}^{(3x3)} \\ \underline{\underline{0}}^{(3x3)} & \underline{\underline{F}}_1^{(3x3)} \end{bmatrix}_{6x6} \qquad (2.113)$$

2.5.4 Three-Node Formulation and General Matrix Form

Three-node matrix form is

$$\underline{\underline{A}}_3 \underline{J}_3 = \frac{1}{k_{eff}} \underline{\underline{F}}_3 \underline{J}_3 \qquad (2.114)$$

where

$$\underline{\underline{A}}_3 = \begin{bmatrix} & & & \underline{\underline{0}}^{(3x3)} \\ \underline{\underline{A}}_2^{(6x6)} & & -t_2 & 0 & 0 \\ & & -\dfrac{S_{5/2}}{\Sigma_a \Delta S_2} & 0 & 0 \\ & & -n_2 & 0 & 0 \\ & -o_3 & 1 & -p_3 & 0 \\ \underline{\underline{0}}^{(3x5)} & -\dfrac{S_{5/2}}{\Sigma_a \Delta S_3} & \dfrac{S_{5/2}}{\Sigma_a \Delta S_3} & 1 & \dfrac{S_{7/2}}{\Sigma_a \Delta S_3} \\ & -m_3 & 0 & -p_3 & 1 \end{bmatrix}_{9x9} \tag{2.115}$$

$$\underline{J}_3^T = \left[j_{1/2}^+ \quad \phi_1 \quad j_{3/2}^+ \quad j_{3/2}^- \quad \phi_2 \quad j_{5/2}^+ \quad j_{5/2}^- \quad \phi_3 \quad j_{7/2}^- \right] \tag{2.116}$$

$$\underline{\underline{F}}_3 = \begin{bmatrix} \underline{\underline{F}}_1^{(3x3)} & \underline{\underline{0}}^{(3x3)} & \underline{\underline{0}}^{(3x3)} \\ \underline{\underline{0}}^{(3x3)} & \underline{\underline{F}}_1^{(3x3)} & \underline{\underline{0}}^{(3x3)} \\ \underline{\underline{0}}^{(3x3)} & \underline{\underline{0}}^{(3x3)} & \underline{\underline{F}}_1^{(3x3)} \end{bmatrix}_{9x9} \tag{2.117}$$

The implementation of $\underline{\underline{A}}$ matrix in the computer code can be accomplished by comparing $\underline{\underline{A}}$ matrices in one-node (2.101), two-node (2.111) and three-node (2.115) formulations. General matrix form

$$\underline{\underline{A}}_N \underline{J}_N = \frac{1}{k_{eff}} \underline{\underline{F}}_N \underline{J}_N \tag{2.118}$$

where

$$\underline{\underline{A}}_N = \begin{bmatrix} & & & \underline{\underline{0}}^{((3N-6)x3))} \\ \underline{\underline{A}}_{N-1}^{((3N-3)x(3N-3))} & -t_{N-1} & 0 & 0 \\ & -\frac{S_{N-1/2}}{\Sigma_a \Delta S_{N-1}} & 0 & 0 \\ & -n_{N-1} & 0 & 0 \\ -o_N & 1 & -p_N & 0 \\ \underline{\underline{0}}^{(3x(3N-4))} & -\frac{S_{N-1/2}}{\Sigma_a \Delta S_N} \quad \frac{S_{N-1/2}}{\Sigma_a \Delta S_N} & 1 & \frac{S_{N+1/2}}{\Sigma_a \Delta S_N} \\ -m_N & 0 & -p_N & 1 \end{bmatrix}_{3Nx3N} \tag{2.119}$$

$$\underline{J}_N^T = \left[j_{1/2}^+ \quad \phi_1 \quad j_{3/2}^+ \quad j_{3/2}^- \ \ldots\ldots\ldots\ldots \quad j_{N-1/2}^- \quad \phi_N \quad j_{N+1/2}^+ \right] \tag{2.120}$$

$$\underline{\underline{F}}_N = \begin{bmatrix} \underline{\underline{F}}_1^{(3x3)} & \underline{\underline{0}}^{(3x3)} & \ldots\ldots\underline{\underline{0}}^{(3x3)} \\ \underline{\underline{0}}^{(3x3)} & \underline{\underline{F}}_1^{(3x3)} & \ldots\ldots\underline{\underline{0}}^{(3x3)} \\ \vdots & \ddots & \vdots \\ \underline{\underline{0}}^{(3x3)} & \underline{\underline{0}}^{(3x3)} & \ldots\ldots\underline{\underline{F}}_1^{(3x3)} \end{bmatrix}_{3Nx3N} \tag{2.121}$$

2.5.5 General Matrix Equation with Reflective Boundary Condition

Reflective boundary condition is

$$J_{N+1/2} = j_{N+1/2}^+ - j_{N+1/2}^- = 0 \tag{2.122}$$

And (2.122) states that $j_{N+1/2}^+$ is equal to $j_{N+1/2}^-$ at boundary. So, only the equations related with the last node will be changed. This corresponds to last column of $\underline{\underline{A}}$, i.e. A(N,N), A(N-1,N) and A(N-2,N). After some simplification, these equations become

$$j_{N-1/2}^- - o_N j_{N-1/2}^+ - t_N j_{N+1/2}^+ - p_N \phi_N = 0 \tag{2.122}$$

$$\Phi_N + \frac{S_{N-1/2} j_{N-1/2}^-}{\Sigma_a \Delta S_N} - \frac{S_{N-1/2} j_{N-1/2}^+}{\Sigma_a \Delta S_N} = \frac{\nu \Sigma_f}{\Sigma_a k_{eff}} \Phi_N \tag{2.123}$$

$$(1 - n_N) j_{N+1/2}^+ - m_N j_{N-1/2}^+ - p_N \phi_N = 0 \tag{2.124}$$

and $\underline{\underline{A}}$ is

$$\underline{\underline{A}}_N = \begin{bmatrix} & & & \underline{\underline{0}}^{((3N-6)x3))} \\ \underline{\underline{A}}_{N-1}^{((3N-3)x(3N-3))} & -t_{N-1} & 0 & 0 \\ & -\frac{S_{N-1/2}}{\Sigma_a \Delta S_{N-1}} & 0 & 0 \\ & -n_{N-1} & 0 & 0 \\ -o_N & 1 & -p_N & -t_2 \\ \underline{\underline{0}}^{(3x(3N-4))} & -\frac{S_{N-1/2}}{\Sigma_a \Delta S_N} & \frac{S_{N-1/2}}{\Sigma_a \Delta S_N} & 1 & 0 \\ -m_N & 0 & -p_N & 1-n_N \end{bmatrix}_{3Nx3N} \tag{2.125}$$

$\underline{\underline{F}}$ and $\underline{J}$ are the same as before.

2.5.6 Fission Source Iteration in Multigroup Diffusion Equations

The multigroup diffusion equations can be written as

$$\begin{aligned} -\vec{\nabla}.D_1\vec{\nabla}\phi_1 + \Sigma_{R1}\phi_1 &= \frac{1}{k_{eff}}\chi_1 Q \\ -\vec{\nabla}.D_2\vec{\nabla}\phi_2 + \Sigma_{R2}\phi_2 &= \frac{1}{k_{eff}}\chi_2 Q + \Sigma_{S1\to 2}\phi_1 \\ &\vdots \qquad\qquad\qquad \vdots \\ -\vec{\nabla}.D_G\vec{\nabla}\phi_G + \Sigma_{RG}\phi_G &= \frac{1}{k_{eff}}\chi_G Q + \Sigma_{S1\to G}\phi_1 + ... + \Sigma_{S(G-1)\to G}\phi_{G-1} \end{aligned} \tag{2.126}$$

It is assumed that there is no upscattering and fission source is defined as

$$Q(r) = \sum_{g'=1}^{G} \nu_{g'}\Sigma_{fg'}\phi_{g'}(r) \tag{2.127}$$

The spatial dependence of the fission source is identical in each group diffusion equation.

The initial estimates of $Q(r)$ and multiplication eigenvalue k_{eff} are made before first iteration

$$Q(r) \sim Q^{(0)}(r), \qquad \text{and} \qquad k_{eff} \sim k^{(0)} \tag{2.128}$$

Next the first group diffusion equation is solved by using linear system solver subroutines [9]

$$-\vec{\nabla}.D_1\vec{\nabla}\phi_1^{(1)} + \Sigma_{R1}\phi_1^{(1)} = \frac{1}{k_{eff}^{(0)}}\chi_1 Q^{(0)}(r) \tag{2.129}$$

The flux in the first group is calculated and the diffusion equation for the next lowest energy group is solved

$$-\vec{\nabla}.D_2\vec{\nabla}\phi_2^{(1)} + \Sigma_{R2}\phi_2^{(1)} = \frac{1}{k_{eff}^{(0)}}\chi_2 Q^{(0)}(r) + \Sigma_{S1\to 2}\phi_1^{(1)} \tag{2.130}$$

and flux of this group is determined for every nodes. All of the group fluxes are found using this procedure. Diffusion equation corresponds to neutron balance equation, so only RHS of (2.123) is changed with additional scattering source term.

A new fission source can be calculated since $\phi_1^{(1)}$, $\phi_2^{(1)}$,….. $\phi_G^{(1)}$ are known.

$$Q^{(1)}(r) = \sum_{g'=1}^{G} \nu_{g'}\Sigma_{fg'}\phi_{g'}^{(1)}(r) \tag{2.131}$$

And a new value of k_{eff}:

$$k_{eff}^{(1)} = \frac{\int Q^{(1)}(r)d^3r}{\frac{1}{k_{eff}^{(0)}}\int Q^{(0)}(r)d^3r} \tag{2.132}$$

There will always exist a maximum eigenvalue, k_{eff} that is real and positive. The corresponding eigenfunction, cell average fluxes and outgoing partial currents, is unique and nonnegative everywhere within the reactor. It can be demonstrated that this fission source iteration will converge to this positive dominant eigenvalue k_{eff} and the corresponding eigenfunction [5].

At this point one tests the source iteration for convergence, such as by comparing

$$\left|\frac{k_{eff}^{(n+1)} - k_{eff}^{(n)}}{k^{(n+1)}}\right| \overset{?}{<} \varepsilon \tag{2.133}$$

If the changes in $k_{eff}^{(n)}$ are sufficiently small, one assumes that convergence has been achieved, and the iterative procedure is ended. If not, a new fission source is calculated and the iteration continues.

3 NUMERICAL APPLICATIONS

The formulations derived in the previous chapter have been implemented in the NEMR code which is a computer program written in FORTRAN 90. This code and the numerical results obtained from it will be described in this chapter. Also comparison with FEM is made by using the results of a computer program, QFEMR.

3.1 One-group, Bare, Homogeneous Reactor

In this problem, a bare, cylindrical reactor of diameter 7.5cm is considered (Figure 3.1). Zero incoming current boundary condition ($j^- = 0$) is assumed at the surface of this cylinder. Effective multiplication factor of this system is determined using the one group cross sections D=0.65cm, Σ_a=0.12cm^{-1} and $\upsilon\Sigma_f$=0.185cm^{-1}.

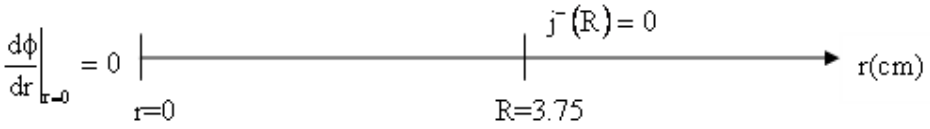

Figure 3.1 One-dimensional, Bare, Homogeneous, Cylindrical Reactor

3.1.1 Analytical Solution

One-group diffusion equation can be written as

$$\frac{1}{r}\frac{d}{dr}r\frac{d\phi(r)}{dr} - \frac{\Sigma_a\phi(r)}{D} = -\frac{1}{k_{eff}}\frac{\nu\Sigma_f}{D}\phi(r) \tag{3.1}$$

Simplifying (3.1)

$$\frac{1}{r}\frac{d}{dr}r\frac{d\phi(r)}{dr} + B^2\phi(r) = 0 \tag{3.2}$$

where B is defined as

$$B^2 = \frac{\frac{\nu\Sigma_f}{k_{eff}} - \Sigma_a}{D} \tag{3.3}$$

Solution of (3.2) is

$$\phi(r) = AJ_0(Br) \tag{3.4}$$

Zero incoming current boundary condition is

$$j^-(R) = \frac{\phi(R)}{4} + \frac{D}{2}\frac{d\phi}{dr}\bigg|_{r=R} = 0 \tag{3.5}$$

Using (3.4) in (3.5) gives

$$J_0(BR) = 2DBJ_1(BR) \tag{3.6}$$

(3.6) can be written as

$$J_0(x) = \frac{2Dx}{R}J_1(x) \tag{3.7}$$

where x=BR. Substituting the numerical values of D and R in (3.7) gives

$$2.884615382J_0(x) - xJ_1(x) = 0 \tag{3.8}$$

(3.8) can be solved by using Newton's Method [10]

$$x^{(t+1)} = x^{(t)} - \frac{f(x^{(t)})}{f'(x^{(t)})} \tag{3.9}$$

where, t is the iteration number. Here f(x) is the left hand side of (3.8). f'(x) can be found using recurrence relation for Bessel Function of first kind,

$$xJ_n' = nJ_n - xJ_{n+1} = -nJ_n + xJ_{n-1} \tag{3.10}$$

Thus, (3.9) becomes

$$x^{(t+1)} = x^{(t)} + \frac{2.884615382J_0(x^{(t)}) - x^{(t)}J_1(x^{(t)})}{2.884615382J_1(x^{(t)}) + x^{(t)}J_0(x^{(t)})} \tag{3.11}$$

Initial estimate of $x^{(0)}$ can be found by assuming critical reactor, k_{eff}=1. In this case, (3.3) gives B=0.316227766 and $x^{(0)}$=BR=1.185854123. Table 3.1 shows the results of Newton's method.

Table 3.1 Iteration Steps of Newton's Method for the Solution of (3.7)

t	$x^{(t)}$	$\varepsilon^{(t)}$ (%)
0	1.185854123	-
1	1.799773445	94.9837
2	1.771173535	1.6145
3	1.771285989	0.0063
4	1.771285991	9.114×10^{-8}

These calculations are made using MATHEMATICA 5.2. Finally, x=1.771285991 and B=x/R=0.47234293cm^{-1}. Effective multiplication factor can be calculated as

$$k_{eff} = \frac{\nu\Sigma_f}{DB^2 + \Sigma_a} = 0.698060264 \tag{3.12}$$

Average flux is defined as

$$\bar{\phi} = \frac{\int_0^R \phi(r) 2\pi r dr}{\pi R^2} \tag{3.13}$$

Average flux can be calculated from (3.13)

$$\bar{\phi} = \frac{2}{R^2} \int_0^R A J_0(0.47234293r) r dr = 0.58086137546A \tag{3.14}$$

In order to find an expression for A, it is necessary to make a separate calculation of the reactor power. In particular, there are $\Sigma_f \phi(r)$ fissions per cm^3/sec at the point of r, and if the recoverable energy is w_f joules per fission (w_f=3.2x10^{-11} joules), then the total power per axial distance, in watts/cm, is

$$P = w_f \Sigma_f \int_0^R \phi(r) 2\pi r dr \tag{3.15}$$

Performing the integration gives

$$P = w_f \Sigma_f \pi R^2 0.58086137546A \tag{3.16}$$

If the reactor power is given as P=2000watt/cm, and the macroscopic fission cross section is Σ_f =0.0764cm^{-1}, then A is calculated as

$$A = \frac{P}{w_f \Sigma_f \pi R^2 0.58086137546} = 3.1894954 \times 10^{13} \tag{3.16}$$

Flux distribution can be found by multiplying constant A with cell average fluxes. Finally, average flux is calculated using (3.16) in (3.14) as

$$\bar{\phi} = 1.852654684 \times 10^{13}\ n^0/cm^2sec. \qquad (3.17)$$

3.1.2 Solution with Nodal Method

Here, formulations derived in previous section are tested with two node calculations before their implementation into the computer program. Figure 3.2 shows the nodes of this system. Since Δ and D are the same for the same material in one-group calculation, τ is the same for two nodes. From (2.73),

τ=12.3152

Δ is calculated by dividing radius, R by the number of nodes, 2. Therefore

Δ=1.875

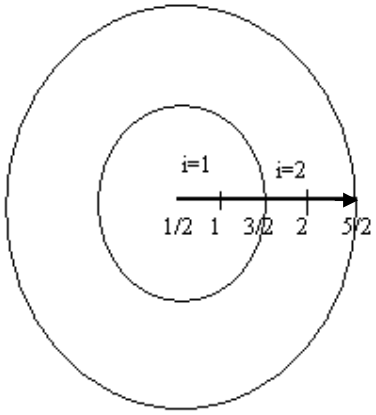

Figure 3.2 Cylindrical Reactor with Two Nodes

Calculated values of the variables describes in (2.76)-(2.80) are given in table 3.2. Radii and corresponding surface areas are given in Table 3.3. They are used in (2.76) through (2.80).

Table 3.2 Calculated Values of the Variables in the Two-Node Equations

i	1	2
m	-0.112598	-0.187663
n	-0.499805	-0.42474
t	-0.337794	-0.262729
o	-0.274609	-0.349674
p	0.403101	0.403101

Table 3.3 Radii and Related Surface Areas

i	r_i (cm)	Si(cm2)
1/2	0	0
1	0.9375	5.8875
3/2	1.8750	11.7750
2	2.8125	17.6625
5/2	3.7500	23.5500

Table 3.2 can be used to test further computer programs which will be developed using nodal methods in cylindrical geometry.

Equations derived in section (2.5.3) are formed. These equations constitute the matrix, A, with numerical values

$$\underline{\underline{A}} = \begin{bmatrix} 1.27461 & -0.403101 & 0 & 0.337794 & 0 & 0 \\ 0 & 1 & 8.88854 & -8.88854 & 0 & 0 \\ 0.112598 & -0.403101 & 1 & 0.499805 & 0 & 0 \\ 0 & 0 & 0.349674 & 1 & -0.403101 & 0 \\ 0 & 0 & -2.96284 & 2.96284 & 1 & 5.92569 \\ 0 & 0 & 0.18663 & 0 & -0.403101 & 1 \end{bmatrix}_{6x6} \tag{3.18}$$

This matrix has 3 upper diagonals and 3 lower diagonals. It is a band matrix. All other A matrices with increased node number have the same character. Therefore, in order to use computer memory economically, only 7 diagonals of these matrices are stored. They are transferred into a new matrix in the NEMR computer program.

All the elements of the matrix F are zero except F(2,2)=F(5,5)=1.541605. Hence, only these elements are used in calculations of NEMR.

If a new matrix defined as

$$\underline{\underline{B}} = \underline{\underline{A}}^{-1}\underline{\underline{F}} \tag{3.19}$$

(2.110) becomes

$$\underline{\underline{A}}^{-1}\,\underline{\underline{F}}\,\underline{J} = \underline{\underline{B}}\underline{J} = k_{eff}\,\underline{J} \tag{3.20}$$

k_{eff} is the maximum eigenvalue of the matrix, B. MATHEMATICA 5.2 first calculates $\underline{\underline{B}}$ using (3.19), then finds the eigenvalues of it. Therefore,

k_{eff}=0.689617 (3.21)

and the error

$$\text{Error}\% = \frac{\left|\text{Analytic}\, k_{eff} - \text{Nodal}\, k_{eff}\right|}{\text{Analytic}\, k_{eff}} \times 100\% = 1.2095\% \quad (3.22)$$

This is a reasonable error as will be shown in the following section.

3.1.3 NEMR and QFEMR Results

Linear FEM, quadratic FEM and NEM results of multiplication factor are given in Table 3.4

Table 3.4 k_{eff} Results of QFEMR and NEMR Programs

Method	Number of Elements(FEM) or Nodes(NEM)	k_{eff}	Error (%)
Linear FEM	2	0.746411132	6.92646
	10	0.699714822	0.23702
	50	0.698125364	0.00933
	100	0.698076062	0.00226
Quadratic FEM	1	0.720881392	3.26922
	2	0.699073117	0.14509
	10	0.698061073	0.0001158
	50	0.698059636	0.00009
Lowest Order NEM	3	0.694169485	0.55737
	5	0.696634106	0.204303
	11	0.697764156	0.042418
	21	0.697979689	0.011543

Quadratic FEM gives better results than linear FEM. In the FEM terminology, the points in the mesh where the unknowns are introduced are called nodes. In the nodal method, a node is not a point, it describes a cell. A linear finite element has two nodes; both are located at the endpoints of the element. Therefore, N elements correspond to N+1 node in the linear FEM. In case of quadratic finite elements, the number of nodes per element increases to three. N quadratic elements contain 2N+1 nodes.

NEM is better than linear FEM. NEM also seems the best method for 3 nodes which corresponds to 1 quadratic element in the quadratic FEM, but then, quadratic FEM gives more accurate results than other methods as shown in figure 3.3.

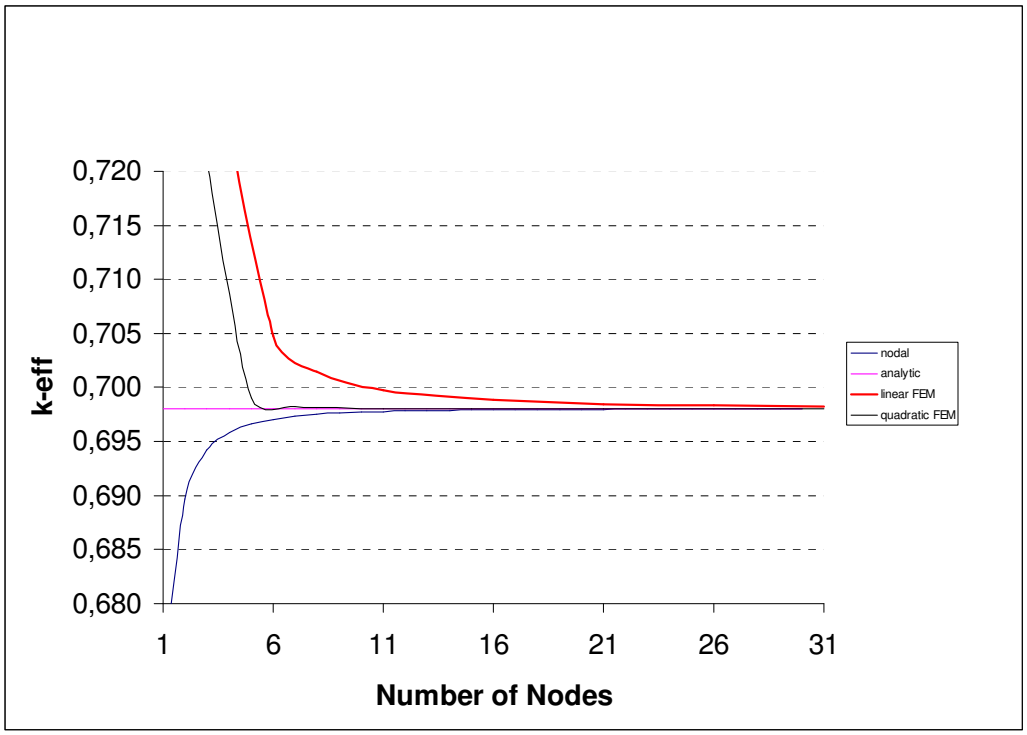

Figure 3.3 k_{eff} Results of FEM and NEM

NEMR code with two nodes gives k_{eff} =0.68963090 with an error 1.20754102%. They are very similar to two-node calculations of k_{eff} (3.21) and its error (3.22). This shows that nodal equations are implemented into the code correctly.

If the number of nodal cells is large, the nodal method loses its calculational advantages with respect to finite element methods. But if the number of nodes are small as 1, 2, 3 nodes, nodal method seems more advantageous than finite element methods as seen in figure 3.3.

(3.13) can be discretized as

$$\bar{\phi} = \frac{\sum_{i=1}^{N} \phi_i S_i}{\sum_{i=1}^{N} S_i} \tag{3.23}$$

NEMR calculates average flux using (3.23). They are given in table 3.5 with linear FEM results. Comparison with exact average flux, (3.17), shows that NEMR is able

to calculate average flux with very little error. The same average flux and therefore the same error are found in linear FEM independently from the number of linear elements. Therefore, only results for 2 and 10 linear elements are given in the table 3.5. Double precision is used as the computer numbering format for the calculation of these fluxes and 9 digits after the decimal point are placed in the table.

Table 3.5 Average Fluxes and Respective Errors

Method	Number of Elements(FEM) or Nodes(NEM)	$\bar{\phi}\times10^{-13}$ ($n^0/cm^2sec.$)	Error (%)
Nodal	3	1.851715510	0.050693418
	5	1.851715485	0.050694768
	11	1.851715342	0.050702486
	21	1.851715253	0.050707290
Linear FEM	2	1.851715400	0.050699356
	10	1.851715400	0.050699356

NEMR can calculate cell average fluxes with small error. Flux distributions are given in figure 3.4 for 31 nodes in NEM which corresponds to 30 linear elements and 15 quadratic elements in QFEMR.

It is shown in figure 3.4 that both NEM and linear FEM graphs are superimposed. Maximum flux is approximately $2.83x10^{13}n^0/cm^2sec$ at the center of the cylinder when the reactor power is taken to be 2000 W/cm.

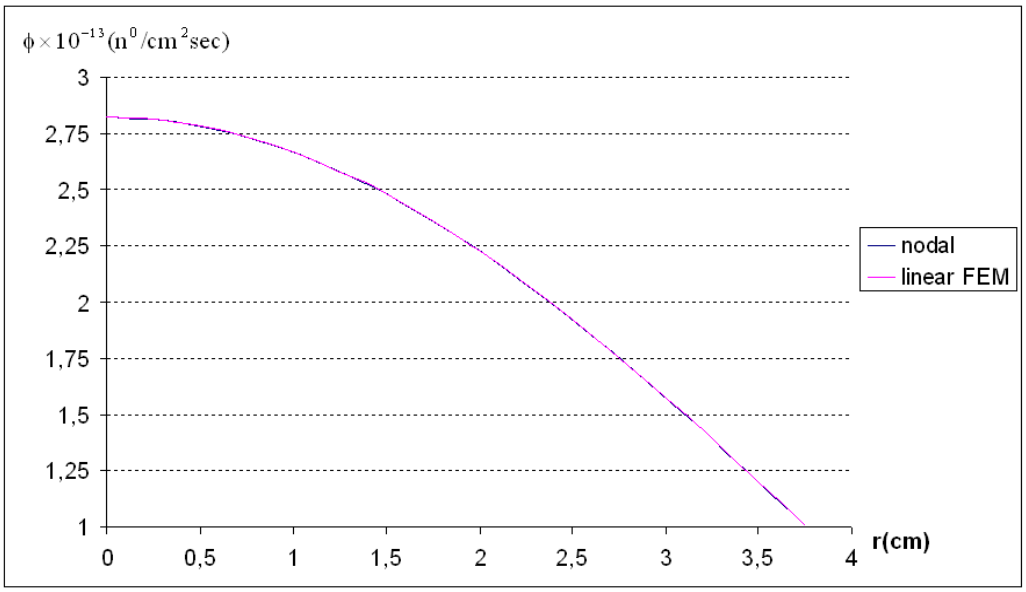

Figure 3.4 Flux Distribution Along the Radial Distance

3.2 One-Group Reflected Reactor

In this section, two-region cylindrical reactor is considered. It is composed of a central cylinder of one fuel-bearing material (region 1) embedded in an annulus of a second reflector material (region 2). It is assumed that multigroup spectra have been determined for the different (nuclearly homogeneous) materials in regions (1) and (2) and that the one-group cross-sections have been obtained by averaging over these spectra.

Fuel-bearing material is the same with the material defined in section 3.1. It has the same cross-sections and the same radius, R_1=3.75cm.

Reflector is a graphite material with thickness 1.25cm. Hence R_2=5cm. Absorption cross-section and diffusion coefficient of the graphite are taken to be 0.00032cm^{-1} and 0.84cm respectively.

3.2.1 Analytical Solution

The resulting form of the one-group diffusion equation is thus

$$D^k\left(\frac{1}{r}\frac{d}{dr}r\frac{d}{dr}\phi(r)\right)+\left(\frac{1}{\lambda}\nu\Sigma_f^k-\Sigma_a^k\right)\phi(r)=0 \tag{3.24}$$

Continuity and boundary conditions are

$$\phi(R_1)^- = \phi(R_1)^+ \tag{3.25}$$

$$D^{(1)}\left.\frac{d\phi(R_1)}{dr}\right|^- = D^{(2)}\left.\frac{d\phi(R_1)}{dr}\right|^+ \tag{3.26}$$

$$\frac{1}{4}\phi(R_2)+\frac{D^{(2)}}{2}\frac{d}{dr}\phi(R_2)=0 \tag{3.27}$$

where R_1 and R_2 are the radii of the fuel-bearing material and the reflector respectively. If one defines

$$(\kappa^k)^2=\frac{\lambda^{-1}\nu\Sigma_f^k-\Sigma_a^k}{D^k}\quad (k=1,2) \tag{3.28}$$

(3.24) can be written as:

$$\left(\frac{1}{r}\frac{d}{dr}r\frac{d}{dr}\phi(r)\right)+(\kappa^k)^2\phi(r)=0 \tag{3.29}$$

Note that, (κ^k) can be real or pure imaginary depending on the magnitudes of the reactor parameters. It takes the form

$$(\kappa^F)^2 = \frac{\lambda^{-1}\nu\Sigma_f^F - \Sigma_a^F}{D^F} \qquad \text{(Fuel region, real)} \tag{3.30}$$

$$(\kappa^R)^2 = \frac{\Sigma_a^R}{D^R} \qquad \text{(Reflector region, imaginary)} \tag{3.31}$$

κ^F is real if $\lambda^{-1}\nu\Sigma_f^F \geq \Sigma_a^F$. Therefore, $\lambda \leq (\nu\Sigma_f^F / \Sigma_a^F = 1.54)$. Since the reflector can not increase the effective multiplication factor so much, the solution in the fuel region is

$$\phi_F(r) = C_1 J_0(\kappa^F r) \tag{3.32}$$

where J_0 is the zeroth-order Bessel function of the first kind. For the reflector region

$$\phi_R(r) = C_3 I_0(\kappa^R r) + C_4 K_0(\kappa^R r) \tag{3.33}$$

where I_0 and K_0 are zeroth-order modified Bessel functions of the first and second kind respectively. Applying zero incoming current boundary condition (3.27) to the (3.33) gives

$$C_3 = -C_4\left[\frac{K_0(\kappa^R R_2) - 2D^R\kappa^R K_1(\kappa^R R_2)}{I_0(\kappa^R R_2) + 2D^R\kappa^R I_1(\kappa^R R_2)}\right] = -C_4 L \tag{3.34}$$

(3.33) becomes

$$\phi_R(r) = C_4(-LI_0(\kappa^R r) + K_0(\kappa^R r)) \tag{3.35}$$

The continuity conditions at r=R_1, (3.25) and (3.26) now require that

$$C_1 J_0(\kappa^c R_1) = C_4(-LI_0(\kappa^R R_1) + K_0(\kappa^R R_1)) \tag{3.36}$$

$$-C_1 D^c \kappa^c J_1(\kappa^c R_1) = C_4 D^R(-L\kappa^R I_1(\kappa^R R_1) - \kappa^R K_1(\kappa^R R_1)) \tag{3.37}$$

The critical equation may be obtained by dividing the first equation (3.36) into the second (3.37)

$$\frac{J_0(\kappa^c R_1)}{D^c\kappa^c J_1(\kappa^c R_1)} = \frac{-LI_0(\kappa^R R_1) + K_0(\kappa^R R_1)}{D^R(L\kappa^R I_1(\kappa^R R_1) + \kappa^R K_1(\kappa^R R_1))} \tag{3.38}$$

RHS of (3.38) is calculated using MATHEMATICA 5.2

$$\frac{J_0(\kappa^c R_1)}{D^c \kappa^c J_1(\kappa^c R_1)} = 2.7822129453 \tag{3.39}$$

(3.39) can be re-arranged as

$$J_0(\kappa^c R_1) - 1.8084384144\,\kappa^c J_1(\kappa^c R_1) = 0 \tag{3.40}$$

(3.40) would be suitable for the Newton's Method, if it is written as

$$f(x) = J_0(x) - 0.482250243 x J_1(x) = 0 \tag{3.41}$$

where $x = \kappa^c R_1$.

Newton's Method, (3.9), takes the form

$$x^{(t+1)} = x^{(t)} + \frac{J_0(x^{(t)}) - 0.482250243 x^{(t)} J_1(x^{(t)})}{J_1(x^{(t)}) + 0.482250243 x^{(t)} J_0(x^{(t)})} \tag{3.42}$$

Table 3.6 shows the steps of this iteration process, (3.42)

Table 3.6 Iteration Results of Newton Method

t	$x^{(t)}$	$\varepsilon^{(t)}(\%)$
0	1	40.599315
1	1.683482	4.13843
2	1.61658	0.0276963
3	1.61703	9.32603×10^{-7}
4	1.61702907	1.37316×10^{-14}

Thus

$$\kappa^c = \frac{x}{R_1} = 0.431207753 \tag{3.43}$$

Effective multiplication factor is found analytically from (3.43) as

$$\lambda = k_{eff} = 0.768077605 \tag{3.44}$$

From (3.13) and (3.15) average flux is

$$\bar{\phi} = \frac{P}{w_f \Sigma_f \pi R_1^2} \tag{3.45}$$

Average flux in the fuel region is the same as calculated in section (3.1.1) and given in (3.17). $\bar{\phi}_F = 1.852654684 \times 10^{13}\ n^0/cm^2 sec$, since all variables of (3.45) remains the same.

But, it is complicated to find the average flux in the reflector. First, it is necessary to find C_1 in (3.32)

$$\bar{\phi}_F = \frac{2}{R_1^2}\int_0^{R_1} C_1 J_0(0.431207753r)rdr \tag{3.46}$$

This integral is evaluated by using the following recursion formula

$$\int x^n J_{n-1}(x)dx = x^n J_n(x) \tag{3.47}$$

Thus

$$\bar{\phi}_F = 0.706884906C_1 \tag{3.48}$$

From (3.17)

$$C_1 = 2.620871754\times 10^{13} \tag{3.49}$$

Next, C_4 is found from (3.36)

$$C_4 = \frac{C_1 J_0(\kappa^c R_1)}{(-LI_0(\kappa^R R_1) + K_0(\kappa^R R_1))} = 1.87991806 \tag{3.50}$$

Average flux in the reflector is defined as

$$\bar{\phi}_R = \frac{\int_{R_1}^{R_2} \phi_R(r)2\pi rdr}{\pi(R_2^2 - R_1^2)} \tag{3.51}$$

Substituting (3.35) into (3.51)

$$\bar{\phi}_R = \frac{2C_4}{(R_2^2 - R_1^2)}\left[-\int_{R_1}^{R_2} LI_0(\kappa^R r)rdr + \int_{R_1}^{R_2} K_0(\kappa^R r)rdr\right] \tag{3.52}$$

These integrals are evaluated using the following recursion formulas

$$\int x^n I_{n-1}(x)dx = x^n I_n(x) \text{ and } \int x^n K_{n-1}(x)dx = -x^n K_n(x) \tag{3.53}$$

Final equation for the average flux in the reflector is

$$\bar{\phi}_R = \frac{-2C_4}{(R_2^2 - R_1^2)(\kappa^R)^2}(L\kappa^R R_2 I_1(\kappa^R R_2) - L\kappa^R R_1 I_1(\kappa^R R_1) + \kappa^R R_2 K_1(\kappa^R R_2) - \kappa^R R_1 K_1(\kappa^R R_1)) \tag{3.54}$$

Average flux has been calculated from (3.54) using MATHEMATICA 5.2

$$\bar{\phi}_R = 8.728700636172 \times 10^{12}\, n^0/cm^2 sec. \quad (3.55)$$

3.2.2 NEMR and QFEMR Results

Table 3.7 shows the effective multiplication factors with their errors. As in the case of previous problem when the node cells are large i.e. with 3 and 5 nodes; NEM gives the best results. The increase of the nodes in the fuel region improves k_{eff} value more than the reflector, since the fuel region is a multiplier medium for neutrons.

Table 3.7 Effective Multiplication Factors Calculated by 3 Methods

Number of Nodes, NEM			**k_{eff}**	**Error (%)**
Fuel	**Reflector**	**Total**		
2	1	3	0.76390350	0.54344834
3	2	5	0.76581560	0.29450214
4	3	7	0.76673990	0.17416274
6	3	9	0.76756920	0.06619188
7	4	11	0.76767430	0.05250837
Linear FEM			**k_{eff}**	**Error (%)**
Fuel	**Reflector**	**Total**		
1	1	3	0.99030426	28.9328382
2	2	5	0.80352910	4.61561344
4	2	7	0.77568958	0.99104196
5	3	9	0.77290074	0.62794903
7	3	11	0.77046017	0.31019905
Quadratic FEM			**k_{eff}**	**Error (%)**
Fuel	**Reflector**	**Total**		
1	1	5	0.78547520	2.26508252
2	1	7	0.76887844	0.10426505
2	2	9	0.76888222	0.10475721
3	2	11	0.76822594	0.01931299
4	2	13	0.76812242	0.00583464

When the number of nodes is 7, quadratic FEM is better than NEM, but if it is 9, NEM seems better unexpectedly. Number of nodes in the fuel region is larger than the reflector region in NEM. But, quadratic FEM puts the same number of elements, 2, into both regions although the total number of nodes is the same in both methods. Therefore, NEM gives more accurate result than quadratic FEM since fuel region is responsible for the neutron multiplication.

After 9 nodes, quadratic FEM gives better results than other two methods. It has been seen that NEM and quadratic FEM have always been better methods than linear FEM for all nodes.

As a result of these considerations, it can be said that nodal method is more advantageous than linear and quadratic FEMs, if the mesh is coarse. When the mesh is getting finer, number of nodes is increased and quadratic FEM becomes more advantageous than other methods. This is shown in figure 3.5.

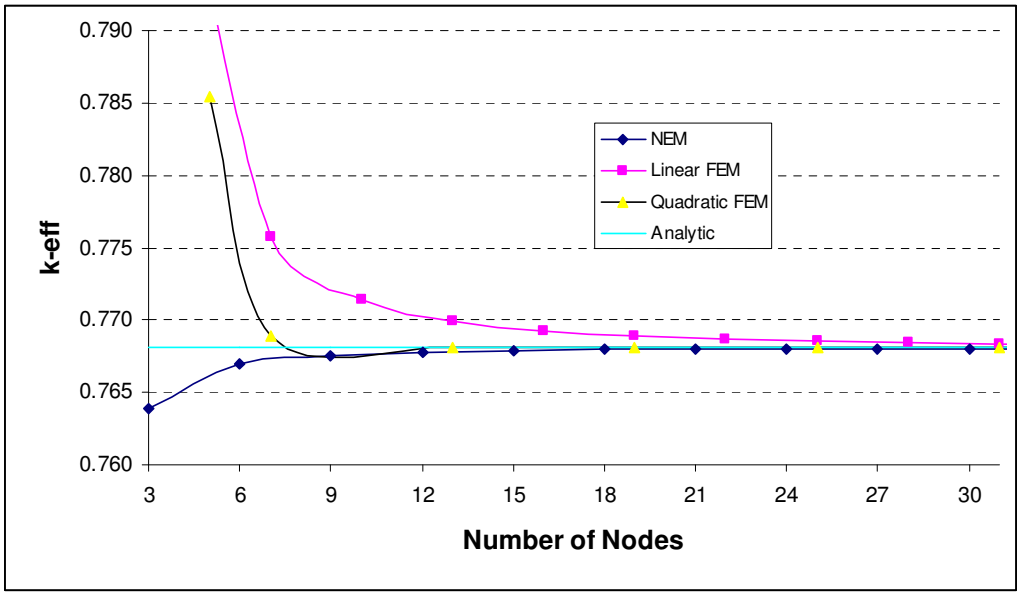

Figure 3.5 Variation of k_{eff} with Respect to Total Number of Nodes

Here, number of elements (nodes) in the fuel region is two times the number of elements (nodes) in the reflector region in FEM (NEM). In the basic mesh there are 2 and 1 nodes in the fuel and the reflector respectively. By multiplying the number of nodes with an integer (which is called degree of refinement) finer meshes are obtained. For example, if the degrees of refinements are 1, 2, 3, 4 and 5; then the number of node ratios in fuel and reflector will be (2:1), (4:2), (6:3), (8:4) and (10:5) respectively.

Mesh refinement is an important tool for editing meshes in order to increase the accuracy of the solution. Refinement is performed in an iterative procedure in which a solution is found, error estimates are calculated, and elements in regions of high error are refined. This process is repeated until the desired accuracy is obtained.

If the total number of nodes is chosen a constant value 33, the optimum number of nodes in the fuel and reflector are found to be 26 and 7 respectively in this problem. So the best rate for the degree of refinement is 26:7. Therefore, optimum mesh spacing or widths of the nodes are calculated as Δ_1=0.14423cm in the fuel and Δ_2=0.17857cm in the reflector.

Quadratic elements seem to be more stable and less influenced to the degree of refinement of the mesh.

Figure 3.6 shows the k_{eff} values from degree of refinement 1 (2:1) to 11 (22:11) for NEM and linear FEM and 6 (12:6) for quadratic FEM. Quadratic FEM seems the same as analytical result since the basic mesh (2:1) corresponds to 7 nodes in quadratic FEM in which its error is very small.

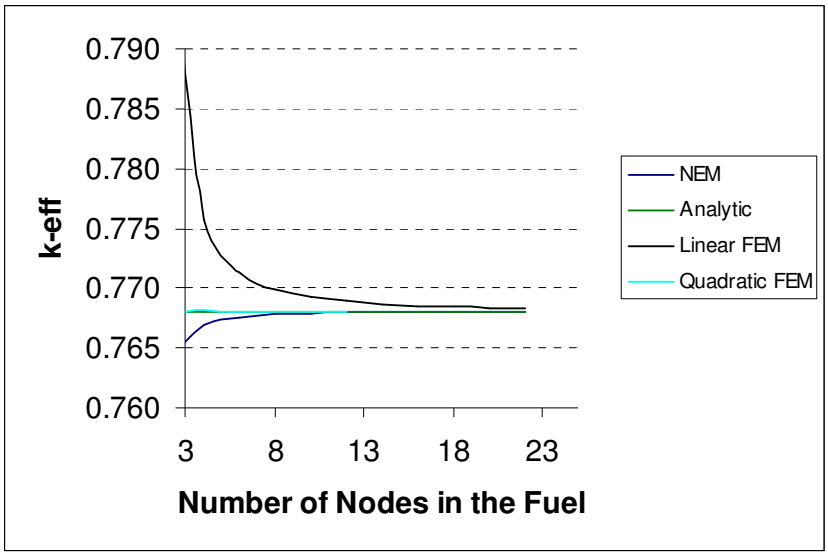

Figure 3.6 k_{eff} versus Number of Nodes in the Fuel Region

Table 3.8 shows the average fluxes calculated in the fuel and the reflector regions. Both methods calculate average fluxes accurately in the fuel region with very small and similar error values. In the reflector, NEMR gives 13.5 times (error ratios) better result for 5 nodes than linear QFEMR for 4 elements which corresponds to 5 nodes. Then, NEMR is still better than linear QFEMR. But linear QFEMR is getting closer to the analytical solution more rapidly. As a result, both methods find the average fluxes with smaller errors when the number of nodes is increased.

Table 3.8 Average Fluxes with Their Errors in The Fuel and The Reflector

	Number of Nodes			$\bar{\phi}_F$ x10^{-13}	Error (%) (Fuel)	$\bar{\phi}_R$ x10^{-13}	Error (%) (Reflector)
	Fuel	Reflector	Total				
NEM	3	2	5	1.851715477	0.050695200	0.878367521	0.629813968
	7	3	10	1.851715418	0.050698385	0.873525390	0.075077163
	14	6	20	1.851715457	0.050696280	0.872703571	0.019074193
	20	10	30	1.851715756	0.050680141	0.872564972	0.034952673
	Number of Elements						
	Fuel	Reflector	Total				
Linear FEM	2	2	4	1.851715400	0.050699336	0.798289649	8.544274488
	6	3	9	1.851715400	0.050699336	0.866251779	0.758221061
	13	6	19	1.851715400	0.050699336	0.871193009	0.192131084
	19	10	29	1.851715400	0.050699336	0.871814416	0.120939875

In figure 3.7, flux distribution along the radius of the cylinder are shown for 30 nodes, 20 fuel and 10 reflector, which corresponds to 29 linear elements. It is seen that two graphs overlap in the figure. Hence, two methods find about the same fluxes.

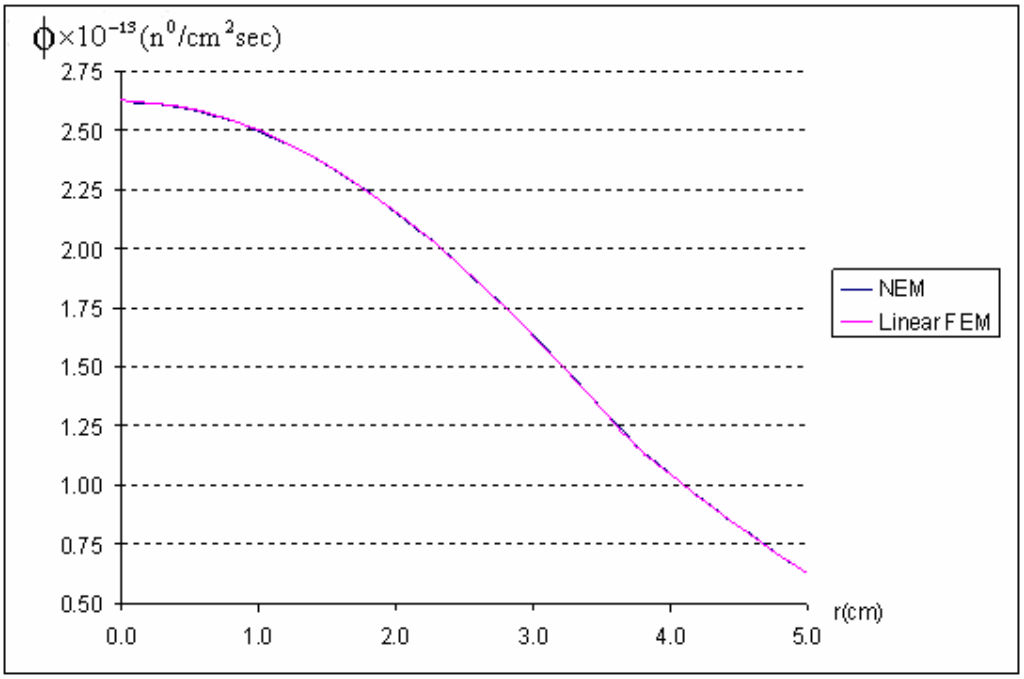

Figure 3.7 Flux Distribution in the Reflected Reactor

3.3 Two-group, Bare, Homogeneous Reactor

In this problem, two-group analysis of a bare, cylindrical reactor is developed. First, critical radius is calculated for zero incoming current boundary condition. Then,

QFEMR and NEMR results are compared to see how close they can calculate k_{eff} to critical value. Two-group parameters are given as

D_1=1.2627cm, Σ_{R1}=0.02619cm^{-1}, $\Sigma_{S,1\to2}$=0.01412cm^{-1}, $\nu_1\Sigma_{f,1}$=0.008476cm^{-1}, D_2=0.3543cm, $\Sigma_{a,2}$=0.1210cm^{-1}, $\nu_2\Sigma_{f,2}$=0.18514cm^{-1} and χ_1=1, χ_2=0.

Reactor power is taken to be 2000W/cm as in the previous problems.

3.3.1 Analytical Solution

Two-group diffusion equations can be written as

$$-\vec{\nabla}.D_1\vec{\nabla}\phi_1+\Sigma_{R1}\phi_1=\frac{1}{k_{eff}}\left[\nu_1\Sigma_{f1}\phi_1+\nu_2\Sigma_{f2}\phi_2\right] \tag{3.56}$$

$$-\vec{\nabla}.D_2\vec{\nabla}\phi_2+\Sigma_{a2}\phi_2=\Sigma_{S,1\to2}\phi_1 \tag{3.57}$$

Since the reactor is critical k_{eff} =1. Assuming, thermal to fast flux ratio is constant and defined by

$$S=\frac{\phi_2}{\phi_1} \tag{3.58}$$

using (3.58) in (3.56) and (3.57) gives respectively

$$\frac{1}{r}\frac{d}{dr}r\frac{d\phi_1}{dr}+\frac{\left(\nu_1\Sigma_{f1}+\nu_2\Sigma_{f2}S-\Sigma_{R1}\right)}{D_1}\phi_1=0 \tag{3.59}$$

$$\frac{1}{r}\frac{d}{dr}r\frac{d\phi_2}{dr}+\frac{\left(\Sigma_{S,1\to2}/S-\Sigma_{a2}\right)}{D_2}\phi_2=0 \tag{3.60}$$

Fast and thermal group buckling terms are defined as

$$B_1^2=\frac{\left(\nu_1\Sigma_{f1}+\nu_2\Sigma_{f2}S-\Sigma_{R1}\right)}{D_1} \tag{3.61}$$

$$B_2^2=\frac{\left(\Sigma_{S,1\to2}/S-\Sigma_{a2}\right)}{D_2} \tag{3.62}$$

Solutions of (3.59) and (3.60) are given by

$$\phi_1(r)=C_1J_0(B_1r) \tag{3.63}$$

$$\phi_2(r)=C_2J_0(B_2r) \tag{3.64}$$

Next, applying zero incoming current boundary condition, (3.5) to (3.63) and (3.64) yields

$$J_0(B_1R) = 2B_1D_1J_1(B_1R) \tag{3.65}$$

$$J_0(B_2R) = 2B_2D_2J_1(B_2R) \tag{3.66}$$

(3.65) and (3.66) are solved iteratively using Newton's Method, (3.9). Then

$$f(x) = J_0(x) - 2B_1D_1J_1(x) \tag{3.67}$$

$$f(y) = J_0(y) - 2B_2D_2J_1(y) \tag{3.68}$$

where $x = B_1R$ and $y = B_2R$. Applying Newton's Method to (3.67) and (3.68) gives

$$x^{(t+1)} = x^{(t)} - \frac{\left(J_0(x^{(t)}) - 2B_1D_1J_1(x^{(t)})\right)}{\left(J_1(x^{(t)})(2B_1D_1 - 1) - 2B_1D_1J_0(x^{(t)})\right)} \tag{3.69}$$

$$y^{(t+1)} = y^{(t)} - \frac{\left(J_0(y^{(t)}) - 2B_2D_2J_1(y^{(t)})\right)}{\left(J_1(y^{(t)})(2B_2D_2 - 1) - 2B_2D_2J_0(y^{(t)})\right)} \tag{3.70}$$

Before iteration, initial estimates of buckling terms are needed. From (3.62)

$$S = \frac{\Sigma_{S,1\to2}}{D_2B_2^2 + \Sigma_{a2}} \tag{3.71}$$

First, initial value of B_2 is estimated. Next, this value is used in (3.69) and flux ratio, S is found. Then, S is used in (3.61) and new value of B_1 is found. B_1 and B_2 are used in (3.69) and (3.70). Also, initial x and y values are estimated with initial critical radius. Solution to this problem with zero flux condition at r=R gives the geometric buckling and the critical radius as B=0.05418cm^{-1}, R=44.3889cm [12]. So, initial B_2 and R values are taken to be 0.06cm^{-1} and 42.0cm respectively.

After the first iteration, new values of x and y are found. These inner iterations continue until the differences $x^{(t+1)}$- $x^{(t)}$ and $y^{(t+1)}$- $y^{(t)}$ are less than 10^{-6}. From converged x and y values, radii R_1 and R_2 are found. New B_2 value is estimated using R_1 and R_2, since it is inversely rated with R_2. Outer iteration continues until the difference between R_1 and R_2 is less than 10^{-7}. One outer iteration step contains two inner iteration steps for thermal and fast group equations. Table 3.9 shows the first two, 10th and the last two outer iteration steps.

Table 3.9 Iteration Steps in Two-Group Problem

Step	B1	B2	R1	R2	R1 -R2
1	0.0538777	0.06	42.0489334	39.3658509	2.6830825
2	0.0543778	0.05	41.6380127	47.3828900	5.7448773
10	0.0540664	0.05644	41.8930428	41.8942962	0.0012534
17	0.0540663	0.05644157	41.8931097	41.8931066	3.12286x10-6
18	0.0540663	0.05644157	41.8931096	41.8931096	6.8311x10-8

Critical radius is found as R=41.8931096cm. Inserting B_2 =0.05644157cm^{-1} into the (3.69), then gives thermal to fast flux ratio S=0.116309825.

Average fluxes can be calculated from (3.13)

$$\bar{\phi}_1 = \frac{2}{R^2}\int_0^R C_1 J_0(B_1 r) r dr = 0.4820488124 C_1 \tag{3.72}$$

$$\bar{\phi}_2 = \frac{2}{R^2}\int_0^R C_2 J_0(B_2 r) r dr = 0.4462414984 C_2 \tag{3.73}$$

Assume that average thermal to fast flux ratio is equal to thermal to fast flux ratio:

$$C_2 \cong 0.125642148 C_1 \tag{3.74}$$

C_1 and C_2 can be written as

$$C_1 = \frac{P_1}{w_f \Sigma_{f,1} \pi R^2 0.4820488124} = 3.3591393\times 10^9 P_1 \tag{3.75}$$

$$C_2 = \frac{P_2}{w_f \Sigma_{f,2} \pi R^2 0.446241498} = 1.6633048\times 10^8 P_2 \tag{3.76}$$

Thermal and fast power constitute the total reactor power

$$P_1 + P_2 = 2000 \text{W/cm} \tag{3.77}$$

There are four equations with four unknowns. Solutions are P_1=565.3845886W/cm, P_2=1434.615411W/cm, C_1=18.992055x10^{11}, C_2=2.3862027x10^{11}. Fast and thermal fluxes are found from (3.63) and (3.64) approximately.

$$\phi_1 = 18.992055\times 10^{11} J_0(B_1 r) \qquad \text{and} \qquad \phi_2 = 2.3862027\times 10^{11} J_0(B_2 r) \tag{3.78}$$

3.3.2 NEMR and QFEMR Results

Effective multiplication factor is calculated with very small error as in the case of the previous sections. The QFEMR and NEMR results of effective multiplication factor, k_{eff} and thermal to fast flux ratios, S are given in table 3.10. S is nearly constant as assumed before. As a result, it is seen that both programs successfully find k_{eff} .

Figure 3.8 shows the k_{eff} values with respect to number of nodes. Again quadratic FEM and NEM are better than linear FEM. When the number of nodes is small, NEM seems to be better and then, quadratic FEM becomes a successful method having a small difference from the NEM.

k_{eff} results of the NEM and quadratic FEM converge ~0.9996. Assumption of constant thermal to fast flux ratio may cause this difference. Actually it is not constant but slowly varying. It is the ratio of zeroth order Bessel functions.

$$S = \frac{C_2 J_0(B_2 r)}{C_1 J_0(B_1 r)} = C_3 \frac{J_0(kB_1 r)}{J_0(B_1 r)} \cong C_3 C_4$$

Table 3.10 Results of QFEMR and NEMR Programs for Two-Group Reactor

Method	Number of	k_{eff}	Error	S	Error (%)
Linear FEM	7	1.028537586	2.853759	0.116332898	0.019837
	10	1.013512079	1.351208	0.115647141	0.569757
	20	1.003065418	0.306542	0.115165093	0.984209
	30	1.001166149	0.116615	0.115076868	1.060063
Quadratic FEM	5	0.999908366	0.009163	0.115465162	0.726218
	10	0.999663253	0.033675	0.115673310	0.547258
	15	0.999655302	0.034470	0.115693296	0.530075
	50	0.999654311	0.034569	0.115697384	0.529607
Lowest Order NEM	2	0.990966845	0.903315	0.115348487	0.826681
	11	0.999426275	0.057372	0.115080686	1.056929
	21	0.999611910	0.038809	0.115030297	1.100252
	31	0.999648762	0.035124	0.115017806	1.110991

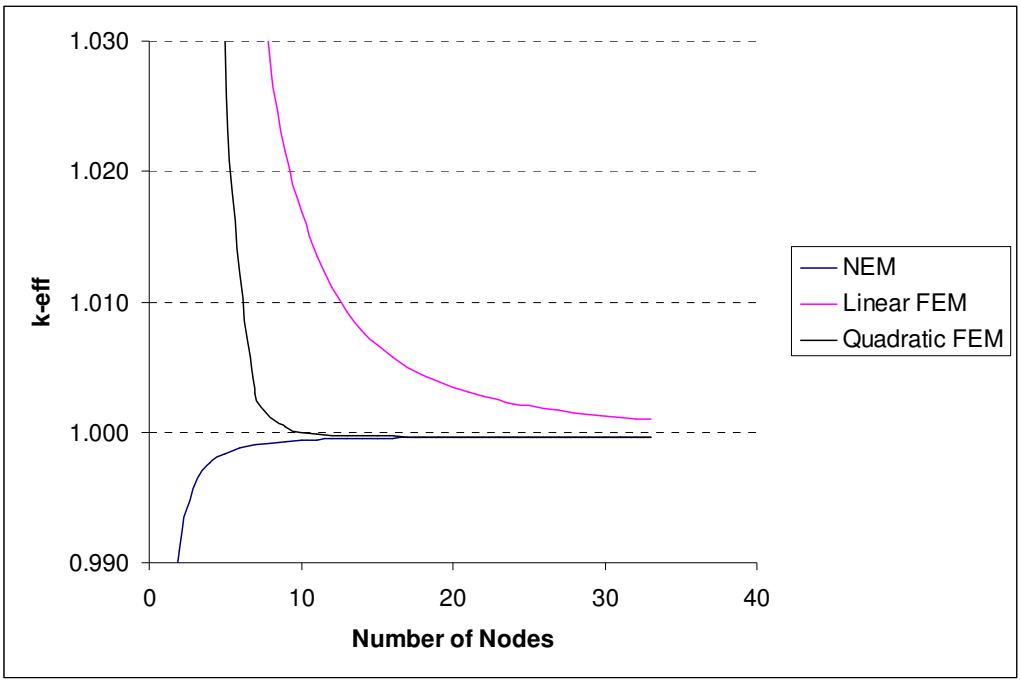

Figure 3.8 Effective Multiplication Factor Obtained by Three Method

Fast and thermal flux distributions can be found from (3.78) analytically. Figure 3.9 shows the fast and thermal fluxes from NEM and analytical method with constant average flux ratio assumption.

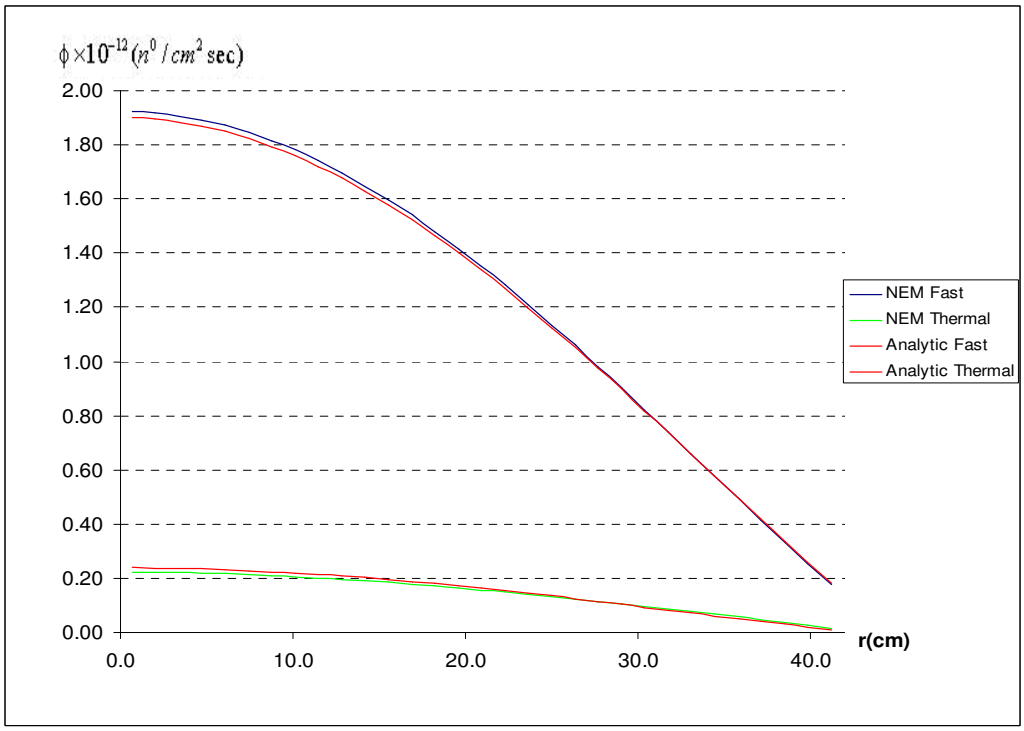

Figure 3.9 Fast and Thermal Flux Distributions

Finally, thermal to fast flux ratios, S, are calculated for 31 nodes. NEM and Quadratic FEM graphs are superimposed as shown in figure 3.10. S values are nearly constant except for the last 2-3 nodes. Average value of S is found to be 0.11418 for all nodes in NEM, but it is 0.11552 when the last two S values for the nodes near the boundary are extracted. When the last four values are extracted, it becomes 0.11567.

Fast and thermal diffusion lengths are calculated as L_1=6.94cm and L_2=1.71cm respectively. Using these values together with buckling terms, nonleakage probabilities are

$$P_{NL_1} = \left(1 + L_1^2 B_1^2\right)^{-1} = 0.8764$$

$$P_{NL_2} = \left(1 + L_2^2 B_2^2\right)^{-1} = 0.9907$$

Amount of fast neutrons is getting higher with respect to the thermal neutrons near the boundary. Therefore, thermal to fast flux ratio, S is lower near the boundary than the inner nodes of this cylindrical reactor.

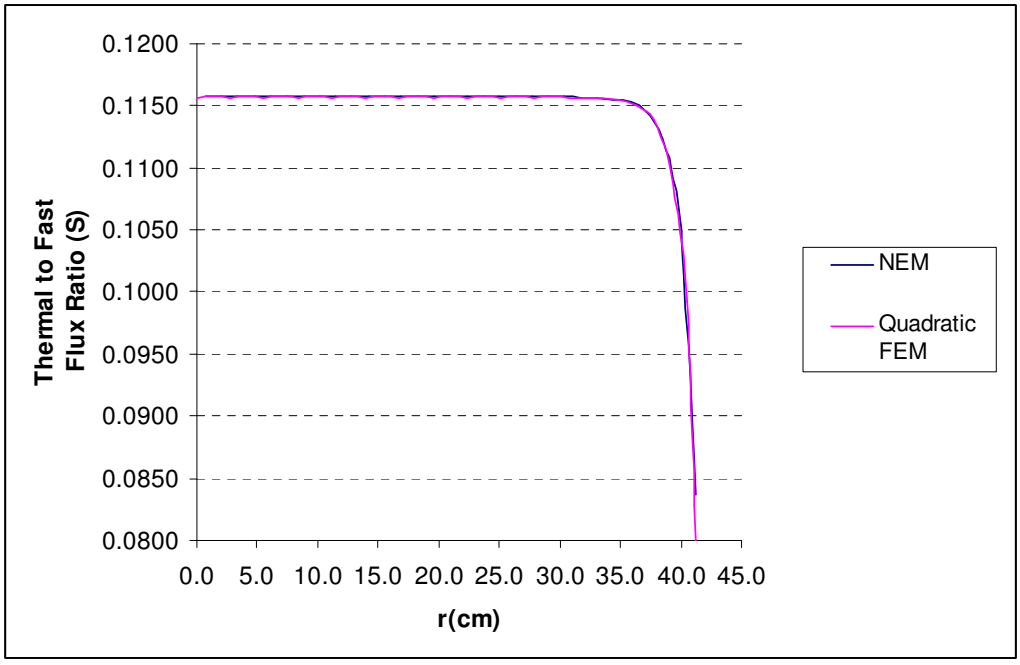

Figure 3.10 Thermal to Fast Flux Ratios Along the Radius

3.4 TRIGA MARK II Reactor

Diffusion theory has been traditionally used for TRIGA whole-core calculations. In this study, one dimensional cylindrical geometry model of TRIGA core is chosen.

Reactor core may be divided into 7 annular regions. Ring A contains only the central thimble. Ring B has 6 fuel elements. Ring C contains 11 fuel elements and one water gap, while ring D has 17 fuel elements and one water gap. Ring E consists of 23 fuel elements and one water gap. Ring F contains 12 fuel elements, 2 water gaps and 16 graphite elements. The core is surrounded by a graphite reflector.

The outer radii of A, B, C, D, E and F rings are 2.1371, 5.9709, 9.8979, 13.8629, 17.7329 and 21.8049 cm's respectively. The graphite reflector outside the F-ring extends to an outer radius of 51.64cm.

The core configuration of the ITU TRIGA MARK II Reactor is given in figure 3.11 [12].

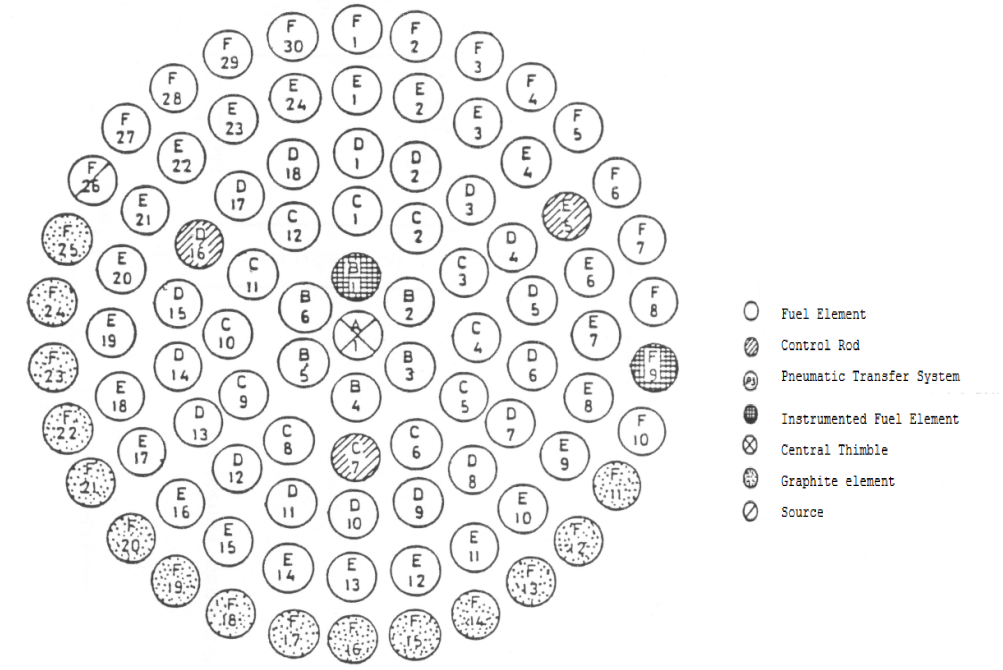

Figure 3.11 ITU TRIGA MARK II Reactor Core Diagram

The homogenized two-group cross-sections for the fuel elements, central thimble, water gap, graphite elements and the graphite reflector has been evaluated using

WIMS-D/4 code in a previous study [13]. These cross-sections are subjected to volume averaged homogenization with:

$$\Sigma_{ring} = \frac{1}{N_{ring}} \sum_{i=1}^{N_{ring}} N_i \Sigma_i \tag{3.79}$$

where N_{ring} represented the total number of cells in a ring; N_i , the number of cells type i in the ring. For the diffusion constant, the volume-averaging is done by:

$$D_{ring} = \frac{N_{ring}}{\sum_{i=1}^{N_{ring}} \frac{N_i}{D_i}} \tag{3.80}$$

After the ring homogenizations are done with (3.79) and (3.80), the following cross-section data are obtained. Table 3.11 and 3.12 shows the homogenized fast and thermal cross-sections respectively.

Table 3.11 Homogenized Fast Group Cross-Sections for TRIGA Reactor

Ring	D_1(cm)	$\Sigma_{r1}(cm^{-1})$	$\Sigma_{s1\rightarrow2}(cm^{-1})$	$\nu_1\Sigma_{f1}(cm^{-1})$
A	1.21848	0.054012	0.053725	0
B	1.01686	0.048046	0.04267	0.00319902
C	1.02952949	0.04861092	0.04365908	0.00293244
D	1.02527139	0.04842261	0.04332939	0.00302130
E	1.02315553	0.04832846	0.04316454	0.00306573
F	1.19993689	0.03345527	0.03123407	0.00127961
Reflector	1.30156	0.002848	0.002845	0

Table 3.12 Homogenized Thermal Group Cross-Sections for TRIGA Reactor

Ring	D_2(cm)	$\Sigma_{a2}(cm^{-1})$	$\nu_2\Sigma_{f2}(cm^{-1})$
A	0.246318	0.01588	0
B	0.244494	0.07921	0.119481
C	0.23985532	0.07394167	0.10952425
D	0.24138186	0.07569778	0.11284317
E	0.24215245	0.07657583	0.11450262
F	0.35853809	0.03561933	0.0477924
Reflector	0.886434	0.000194	0

This data is supplemented with ν_1=2.55, ν_2=2.44, χ_1=1 and χ_2=0. All of them are intended for input to the programs NEMR and QFEMR.

Then, the nodal program NEMR is run with a mesh consisting of 20 nodes. In this basic mesh, there are 1, 2, 3, 3, 3, 2 and 6 nodes in A, B, C, D, E, F rings and the graphite reflector respectively.

NEMR finds the effective multiplication factor as k_{eff}=1.21054283. Linear QFEMR and quadratic QFEMR find k_{eff} =1.21279558 and k_{eff} =1.21052344 with 20 elements respectively.

By multiplying the number of annular regions in the basic mesh by an integer (degree of refinement), finer meshes may be produced. For example, the mesh whose degree of refinement is 4 contains 80 annular regions with 4, 8, 12, 12, 12, 8 and 24 in A, B, C, D, E, F rings and the graphite reflector respectively.

In QFEMR finest mesh consists of 641 nodes which correspond to 640 linear elements and 320 quadratic elements. QFEMR with 320 quadratic elements or 16 degree of refinement gives k_{eff} =1.21051196. Quadratic QFEMR gives more exact results as shown in the previous problems when the number of elements is increased. Therefore, using the finest mesh quadratic QFEMR method, the error in the NEMR result is

$$\text{Error}(\%) = \frac{|1.21051196 - 1.21054283| \times 100\%}{1.21051196} = 0.00255016\%$$

This validates that NEMR can calculate effective multiplication factors of the TRIGA-like two-group, multiregional systems with a small error.

QFEMR with 640 linear elements or 32 degree of refinement (32, 64, 96, 96, 96, 64, 192 annular regions from center to the outside) gives k_{eff} =1.21051424.

Figure 3.12 shows the fast and thermal flux distributions from NEMR. Reactor thermal power is taken to be 1000W/cm. These flux profiles are very similar to the results of before studies [13]. A straight line shows the boundary between the fuel region and the reflector at 21.8 cm.

Figure 3.13 shows linear QFEMR results with 640 elements. NEMR and linear QFEMR flux profiles are very close to each other.

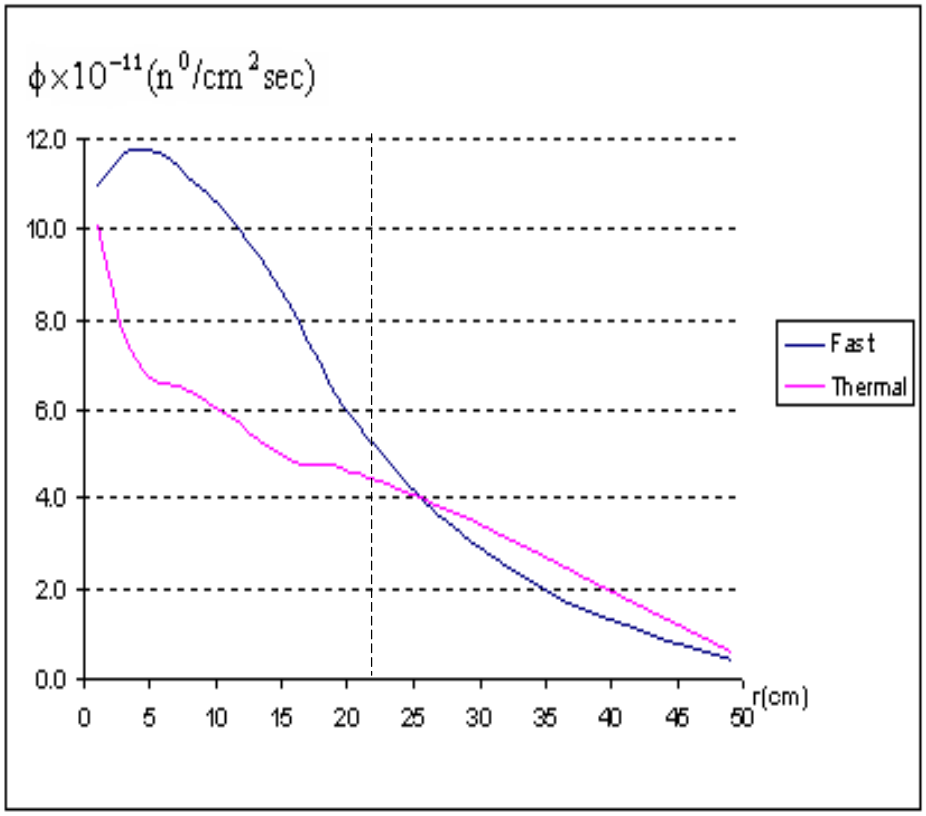

Figure 3.12 TRIGA Reactor Flux Distribution (NEMR)

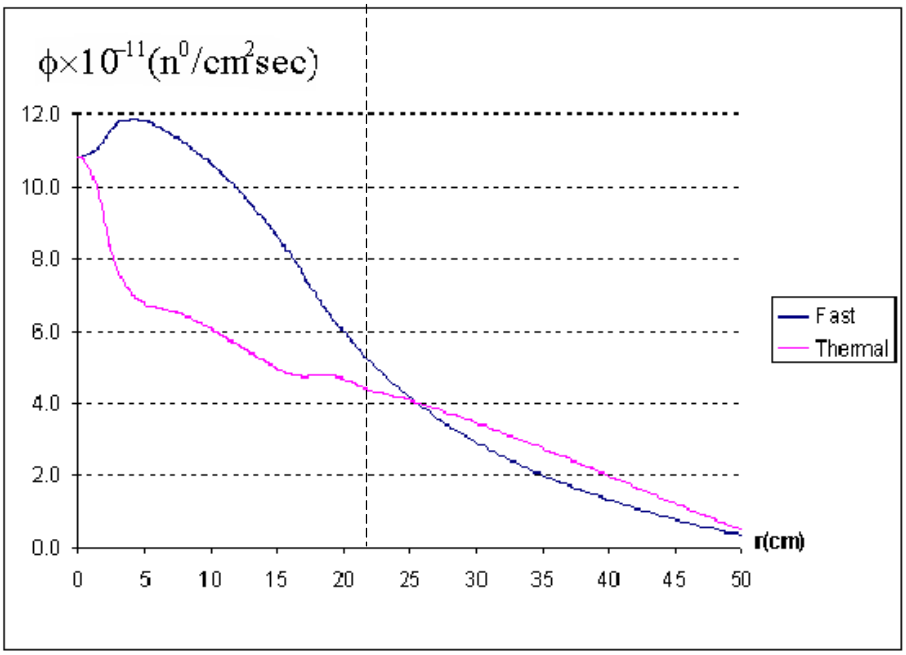

Figure 3.13 TRIGA Reactor Flux Distribution (Linear QFEMR)

Fast and thermal group average fluxes are calculated by NEMR as

Φ_F=0.4599215758x10^{12}neutrons/cm^2sec.

Φ_T=0.3468320710x10^{12}neutrons/cm^2sec.

Finally, ring averaged fluxes are given in table 3.13. Similar results are obtained with the finest mesh linear QFEMR.

Table 3.13 Ring Averaged Fluxes of TRIGA Reactor

Average Fluxes	NEMR		Linear QFEMR	
Ring	Fast Flux $\bar{\phi}_F \times 10^{-11}$	Thermal Flux $\bar{\phi}_T \times 10^{-11}$	Fast Flux $\bar{\phi}_F \times 10^{-11}$	Thermal Flux $\bar{\phi}_T \times 10^{-11}$
A	10.96218643	10.06898070	11.07603868	9.81655374
B	11.73097594	7.076657695	11.74535495	7.07977055
C	11.14299074	6.369204184	11.14005651	6.37756205
D	9.895614128	5.599215700	9.88816852	5.59883768
E	8.131826966	4.847352052	8.11869472	4.84953114
F	6.068752771	4.638547901	6.05777394	4.62723878
Reflector	1.718679834	2.138829250	1.72210595	2.12991548

4 CONCLUSION

In the present work lowest order nodal expansion method in solving neutron diffusion equation in one dimensional cylindrical geometry has been presented and numerically evaluated. Based on the nodal balance equation and Fick's Law, the relationships between the cell averaged flux and partial currents were derived for each node, which can provide efficient formulations for the multigroup and multiregional problems to be solved in a computer program.

The derived formulations have been implemented in the NEMR code which is a FORTRAN 90 program. It can be used for the problems with zero incoming current and reflective boundary conditions. Flux distributions, average fluxes for each group and the material, number of iterations for convergence and the effective multiplication factor are found in the output file. NEMR has been tested with four benchmarking problems with obtained analytical solutions.

First problem was the bare homogeneous reactor and the matrix equation was tested in section (3.1.2) before implementation into the code. Other problems were one-group reflected reactor, two group reactor and TRIGA reactor respectively. Iterative methods have had to be used for finding the analytical solutions because of the transcendental nature of the resulting equations after applying zero incoming current boundary condition. Comparison of analytical and numerical results has shown that NEMR gives accurate results of effective multiplication factor, average fluxes and flux distributions.

A finite element method program, namely QFEMR was used in order to compare nodal expansion method with linear and quadratic finite element methods. NEM and quadratic FEM were shown to be of better accuracy with respect to linear FEM. It also appears that NEM is a practical method for the problems in which the mesh is very coarse (1, 2, 3 nodes etc.). The real power of the nodal approach is realized only when the number of node cells is small, since then the cells are large enough that they become coupled via neutron diffusion only to nearby cells.

For future work, higher order polynomial basis can be constructed. Especially, the cubic polynomial and the quartic polynomial can be formed, since N is rarely chosen greater than 4. But it is not possible to express the coefficients solely in terms of the edged averaged fluxes and the cell averaged flux. It is needed to define flux moments and express the coefficients of the polynomials in terms of them.

Next, one dimensional cylindrical geometry can be expanded two dimensional cylindrical geometry (r-z). Two dimensional partial differential equation can be reduced ordinary differential equations using transverse integration. But in (r-θ) and (r-θ-z) dimensions it fails.

REFERENCES

[1] Lamarsh, J.R., 1983. Introduction to Nuclear Engineering, Addison-Wesley, Reading, Massachusetts.

[2] Stacey, W.M., 2001. Nuclear Reactor Physics, John Wiley and Sons INC., New York.

[3] Duderstadt, J.J. and Hamilton L.J., 1976. Nuclear Reactor Analysis, John Wiley and Sons INC., New York.

[4] Ozgener, H.A. and Ozgener, B., 2007. Advanced Reactor Analysis II, Study Guide For NUCI 875 ET., North-West University.

[5] Finneman, H., Bennewitz, F. and Wagner, M.R., 1977. Interface Current Techniques for Multidimensional Reactor Calculations, Atomkernenergie, 30.

[6] Ougouag, A.M. and Terry, W.K., 2002. Development of a Nodal Method for the Solution of the Neutron Diffusion Equation in General Cylindrical Geometry, *Idaho National Engineering and Environmental Laboratory Technical Report*, INEEL/EXT-02-00489, Idaho Falls, Idaho.

[7] Fisher, H.D. and Finneman H., 1981. The Nodal Integration Method-A Diverse Solver for Neutron Diffusion Problems, .Atomkernenergie-Kerntechnick, 39.

[8] Finneman, H., Bennewitz, F. and Wagner, M.R., 1975. Higher Order Corrections in Nodal Reactor Calculations, Trans. Am. Nuc. Soc., 22.

[9] http://www.netlib.org/linpack/dgbsl.f, http://www.netlib.org/linpack/dgbfa.f

[10] Hoffman, J.D., 2001. Numerical Methods for Engineers and Scientists. Marcel Dekker, Inc., New York-Basel.

[11] Henry, A.F., 1980. Nuclear Reactor Analysis, The Massachusetts Institute of Technology,

[12] Safety Analysis Report for the ITU TRIGA MARK II Reactor. 1978.

[13] Ozgener, H.A., 1999. A comparison of integral transport and diffusion theory methods in whole core TRIGA calculations, *VTT Symposiom,* **197***,* 27-38.

APPENDIX A A MANUAL FOR NEMR

APPENDIX A.1 INPUT LIST

Every line subjected to a single READ command in the input file of NEMR is called a card. Therefore, the input file consists of the following cards:

CARD 1

NGT: Number of energy groups.

MAT: Number of materials.

NETSOR: Free neutron source. It is 1, if the free neutron source exists in the system. It is 0 otherwise.

NRBCT: Boundary condition. It is 1, if the boundary condition is zero incoming current at the boundary. It is 0, if the reflective boundary condition is used.

CARD 2

ITMAX: Maximum number of iterations.

EPS: Convergence parameter.

ENGEN1: Initial estimate of effective multiplication factor.

CARD 3

SKAY(I, J): Free neutron source of I^{th} group and J^{th} material. Every line indicates the material number and every given number in a line is for the energy group of that material. NEMR skips this card if NETSOR is given zero.

CARD 4

D(I,J): Diffusion coefficients for I^{th} group and J^{th} material.

CARD 5

CEKES(I,J): Removal cross-sections for I^{th} group and J^{th} material.

CARD 6

SEKES(I,K,J): Scattering cross-sections from group K to the group I for J^{th} material.

CARD 7

FEKES(I,J): Fission reaction cross-section. $\nu\Sigma_f$ for I^{th} group and J^{th} material.

CARD 8

FEKES1(I,J): Fission cross-section, Σ_f for I^{th} group and J^{th} material.

Card 4,5,6,7 and 8 are repeated for each material.

CARD 9

SFIS(I): Fission spectrum, χ for I^{th} group.

CARD 10

NOD (I): Number of nodes in I^{th} material.

CARD 11

RDIS(I): Outer radius of I^{th} material.

CARD 12

P: Reactor thermal power in Watts/cm.

APPENDİX A.2 DESCRIPTION OF NEMR SUBPROGRAMS

MAIN PROGRAM: ML, MU and M denote band width below diagonal, band width upper diagonal and total diagonals of matrix A formed in subroutine MATRIS. All matrix A formed have the same band width, ML=3, MU=3 and hence M=7 in this nodal formalism. SUM is the total number of nodes and N is the dimension of matrix A which corresponds to number of equations in nodal formalism. Next program segment is for band storage. This uses rows ML+1 through 2xML+MU+1 of ABD. In addition, the first ML rows in ABD are used for elements generated during the triangularization. The total number of rows needed in ABD is 2*ML+MU+1=10. The ML+MU by ML+MU upper left triangle and the ML by ML lower right triangle are not referenced.

After factorization with subroutine DGBF, two dimensional matrix ABD and one dimensional vector IPVT are transferred new three dimensional array ABC and two dimensional array IP, since energy group constitutes extra dimension.

Fission source iteration starts with ITT=0 which is the iteration number. Initial estimates of cell average fluxes and the edge averaged currents are given with the array B2(I,IEG)=1, where IEG denotes the energy group. B2 is the RHS of the matrix equation. After fission source iteration using subroutine FISSOR, CHKEG is tested with the convergence criterion EPS. CHKEG shows the relative difference between two successive effective multiplication factors calculated from iterations.

After adding scattering terms to the B2 with a routine called SCASSOR, linear system is solved with another routine called DGBSL. The solution vector is B, which is equalized B2(I,IEG) for each group. FLUX(I,IEG) consists of cell average fluxes for each node. Then, iteration continues.

Next, these new fluxes are used in the next iteration. At the end of the iterations, converged k_{eff} and fluxes are obtained. Average fluxes and the normalized fluxes with the given power are obtained from the last subroutines.

SKINP: Reads the free source values for each group and the material from the input file.

INPUT: Reads the cross-sections, fission spectrums, number of nodes for each material and the material outer radii from the input file and writes to the output file.

FISSOR: Makes the fission source iteration described in section 2.5.6. S is the vectorial form of Q in (2.126). Initial elements of S are found using the initial estimate of B2 for the first iteration. In the next iterations, B2 is the solution vector from the routine DGBSL. Initial S vector is given as

$$\underline{S}^{(0)} = \begin{bmatrix} 0 \\ (\nu_f \Sigma_f)_1 \phi^{(0),node1}_{group1} + (\nu_f \Sigma_f)_2 \phi^{(0),node1}_{group2} + ... + (\nu_f \Sigma_f)_G \phi^{(0),node1}_{groupG} \\ 0 \\ 0 \\ (\nu_f \Sigma_f)_1 \phi^{(0),node2}_{group1} + (\nu_f \Sigma_f)_2 \phi^{(0),node2}_{group2} + ... + (\nu_f \Sigma_f)_G \phi^{(0),node2}_{groupG} \\ 0 \\ \vdots \\ (\nu_f \Sigma_f)_1 \phi^{(0),nodeN}_{group1} + (\nu_f \Sigma_f)_2 \phi^{(0),nodeN}_{group2} + ... + (\nu_f \Sigma_f)_G \phi^{(0),nodeN}_{groupG} \\ 0 \end{bmatrix} \qquad \text{(A2.1)}$$

FINT corresponds to the numerator of (2.132). FINOR is the integral of the denominator of (2.132). Finally, new B2 vector is the RHS of nodal balance equation without scattering term.

MATRIS: Calculates the elements of matrix A described in the equation (2.125) for the zero incoming current and reflective boundary conditions. All elements of the matrix A were described in section (2.5).

SCASOR: Free source and scattering terms of the nodal balance equation are calculated with this routine. B1 contains these terms. Adding B1 from this routine and B2 from FISSOR constitutes new B2 which is the RHS of matrix equation.

DGBF: Factors a double precision band matrix by elimination. ABD contains the matrix in band storage. The columns of the matrix A are stored in the columns of ABD and the diagonals of the matrix A are stored in rows ML+1 through 2xML+MU+1 of ABD. LDA is the leading dimension of the array ABD. LDA must be greater or equal to 2xML + MU + 1=10.

On return, ABD is an upper triangular matrix in band storage and the multipliers which were used to obtain it. The factorization can be written A = L*U where L is a product of permutation and unit lower triangular matrices and U is upper triangular. IPVT contains the pivot indices.

If info returns info=0, this is the normal value. It equals to k if U(k,k) equals to 0.0. This is not an error condition for this subroutine, but indicates that DGBSL will divide by zero if called.

DGBF calls the subroutines DAXPY and DSCAL and the integer function IDAMAX.

DAXPY: It returns constant times a vector plus a vector. It uses unrolled loops for increments equal to one.

INTEGER FUNCTION IDAMAX: Finds the smallest index of that component of a vector having the maximum magnitude.

DSCAL: Scales a vector by a constant. It uses unrolled loops for increment equals to one.

DGBSL: Solves the double precision band system Ax=B using the factors computed by DGBFA. B is the RHS vector. On return, it gives the solution vector B. It calls subroutine DAXPY.

AVG: Calculates the average fluxes for each material and group. AFLUX is the group averaged flux and AF is material averaged flux.

OUTPUT: First calculates, the constant A described (3.16) for the problem 1. Then, flux distribution with respect to the radius is found. Last, averaged fluxes are written into the output file.

APPENDIX B COMPUTER PROGRAMS

NEMR and QFEMR programs with input files for the problems considered in this study are given in an enclosed CD.

RESUME

He was born in 1976 in Kayseri. He finished the high school in Kayseri Fen Lisesi in 1994. He earned his bachelors degree in Nuclear Energy Engineering in 2003 from Hacettepe University.

He is still working in Istanbul Technical University, Energy Institute.